



**GEOLOGICAL SURVEY OF CANADA
OPEN FILE 7077**

**Downhole geophysical logging and preliminary analyses of
bedrock structural data for groundwater applications
in the Montérégie Est area, Québec**

**H.L. Crow, P. Ladevèze, M. Laurencelle,
N. Benoit, C. Rivard, R. Lefebvre**

2013



Natural Resources
Canada

Ressources naturelles
Canada

Canada



**GEOLOGICAL SURVEY OF CANADA
OPEN FILE 7077**

**Downhole geophysical logging and preliminary analyses of
bedrock structural data for groundwater applications
in the Montérégie Est area, Québec**

**H.L. Crow¹, P. Ladevèze², M. Laurencelle², N. Benoit³, C. Rivard³, R.
Lefebvre²**

¹ Geological Survey of Canada (Ottawa), 601 Booth Street, Ottawa, ON K1A 0E8

² Institut national de la recherche scientifique, 490 rue de la Couronne, Québec, QC G1K 9A9

³ Geological Survey of Canada (Quebec), 490 rue de la Couronne, Québec, QC G1K 9A9

2013

©Her Majesty the Queen in Right of Canada 2013

doi:10.4095/292295

This publication is available for free download through GEOSCAN (<http://geoscan.ess.nrcan.gc.ca/>).

Recommended citation

Crow, H.L., Ladevèze, P., Laurencelle, M., Benoit, N., Rivard, C., and Lefebvre, R., 2013. Downhole geophysical logging and preliminary analyses of bedrock structural data for groundwater applications in the Montérégie Est area, Québec; Geological Survey of Canada, Open File 7077. doi:10.4095/292295

Publications in this series have not been edited; they are released as submitted by the author.

Table of Contents

1.0 Introduction	2
1.1 Regional groundwater study & previous work	2
1.1.1 Joint Groundwater Activity in the Montérégie Est area	2
1.1.2 Geological contexts in the study area	4
1.1.3 Previous downhole geophysical surveys	5
1.1.4 Borehole site selection	5
2.0 Fieldwork	6
2.1 Drilling methods and sample collection	6
2.2 Geophysical logging	8
3.0 Data Analyses	11
3.1 Log data	11
3.1.1 Lithological logs	11
3.1.2 Hydrogeophysical logs	11
3.1.3 Structural logs	12
3.2 Structural data	13
3.2.1 Methodology	13
3.2.2 Results	14
3.2.3 Discussion	20
4.0 Conclusions & Recommendations	21
4.1 Influence of the drilling method and borehole depth on structural dataset	21
4.2 Downhole logging results	21
4.3 Structural analyses	22
5.0 Future Research	22
6.0 Acknowledgements	23
7.0 References	24
Appendix I – Geophysical Log Background	i
Gamma Methods	i
Electromagnetic Induction Methods	i
Fluid Logging Methods	ii
Imaging Methods	iv
Appendix II – Geophysical Logs	v
Appendix III – Structural Classifications	xviii
Digital Appendix IV – Flowmeter Summaries	
Digital Appendix V – Log Data (.LAS files)	

1.0 Introduction

To support the Montérégie Est regional aquifer characterization study, carried out in partnership by the Geological Survey of Canada (GSC) and the Institut national de la recherche scientifique - Centre Eau Terre Environnement (INRS-ETE), downhole geophysical logging was conducted during the fall of 2011 in twelve boreholes located in between Montreal, Sherbrooke, and Drummondville, QC. The objective of the logging was to provide the Montérégie Est groundwater activity with a high-quality dataset of downhole geophysical and hydrogeological information. The *in situ* measurements of bedrock fracture orientation and flowmeter readings represent an important element of this dataset, as they contribute to a better understanding of the structural controls on the hydraulic properties of the regional rock aquifer. Fractures in sedimentary and low-grade metamorphic rocks of low hydraulic conductivity, such as those in the Montérégie Est study area, are expected to have a major influence on flow, as they typically represent the main pathway for groundwater movement in rock aquifers.

The following report outlines the fieldwork and data analyses carried out in four new wells drilled during the project's Phase II drilling in 2011. It also includes data from the re-logging of eight Phase I boreholes drilled in 2010. The analysis of structural data resulting from the interpretation of twelve acoustic televiewer images is presented along with a discussion summarizing the results of the logging, recommendations for future work, and topics of ongoing research.

1.1 Regional groundwater study & previous work

1.1.1 Joint Groundwater Activity in the Montérégie Est area

Aquifers of the Yamaska and Richelieu/Lake Champlain watersheds (including Missisquoi Bay) are being characterized within the groundwater mapping program of the GSC and the "Programme d'acquisition de connaissances sur les eaux souterraines du Québec" (PACES; MDDEFP, 2008a; MDDEFP, 2008b). PACES is a systematic groundwater resource assessment program initiated in 2008 by the Environment Ministry of Québec (Ministère du Développement durable, de l'Environnement, de la Faune et des Parcs du Québec, MDDEFP) which aims to characterize and protect the groundwater and aquifers of the main populated regions in the province of Québec. Within the GSC and PACES' Montérégie Est project, efficient multidisciplinary characterization approaches were developed using geological, geophysical, geochemical, and hydraulic methods. The downhole geophysical datasets are a key component of this integrated aquifer characterization.

The study area covers about 9 000 km² in Québec and 7 500 km² in the United States, extending from the St. Lawrence River southward to Vermont and New York states. This hydrogeological system had been prioritized by the GSC due to its relatively large population and water demand, as well as its transboundary status. In the study area on the Québec side, the population averages 577 000 inhabitants, 26% of whom use groundwater as their water supply. In the study area on the U.S. side, 50% of the 75 000 inhabitants in New York State and 80% of the 63 000 inhabitants in Vermont State use this resource for their supply. In these areas, bedrock is the main regional aquifer, although local aquifers can be found in surficial sediments, such as fluvio-glacial deposits (e.g. eskers).

Limited data are available on the U.S. side, and no fieldwork is currently being carried out. Therefore, this Open File focuses only on the Canadian portion of the study area (the Montérégie Est area), which is located east of Montreal, extending from Sorel in the north, down to the U.S. border. Figure 1

illustrates the three watersheds (Richelieu, Yamaska and Missisquoi Bay), along with regional municipalities (*Municipalités régionales de comté, MRC*), main municipalities, and rivers.

The geophysical logging carried out as part of this study complements other fieldwork, which has included direct push soundings (Cone Penetration Tests, CPT, and soundings with a Rotopercussion Sounding System, RPSS) into surficial sediments and drilling into bedrock, water and soil sampling, as well as permeameter testing to measure hydraulic conductivity (K) in sediments. Additional geophysical surveys have included surface seismic, time domain electromagnetic (TDEM), electrical resistivity and ground penetrating radar (GPR) to better understand the local stratigraphy.

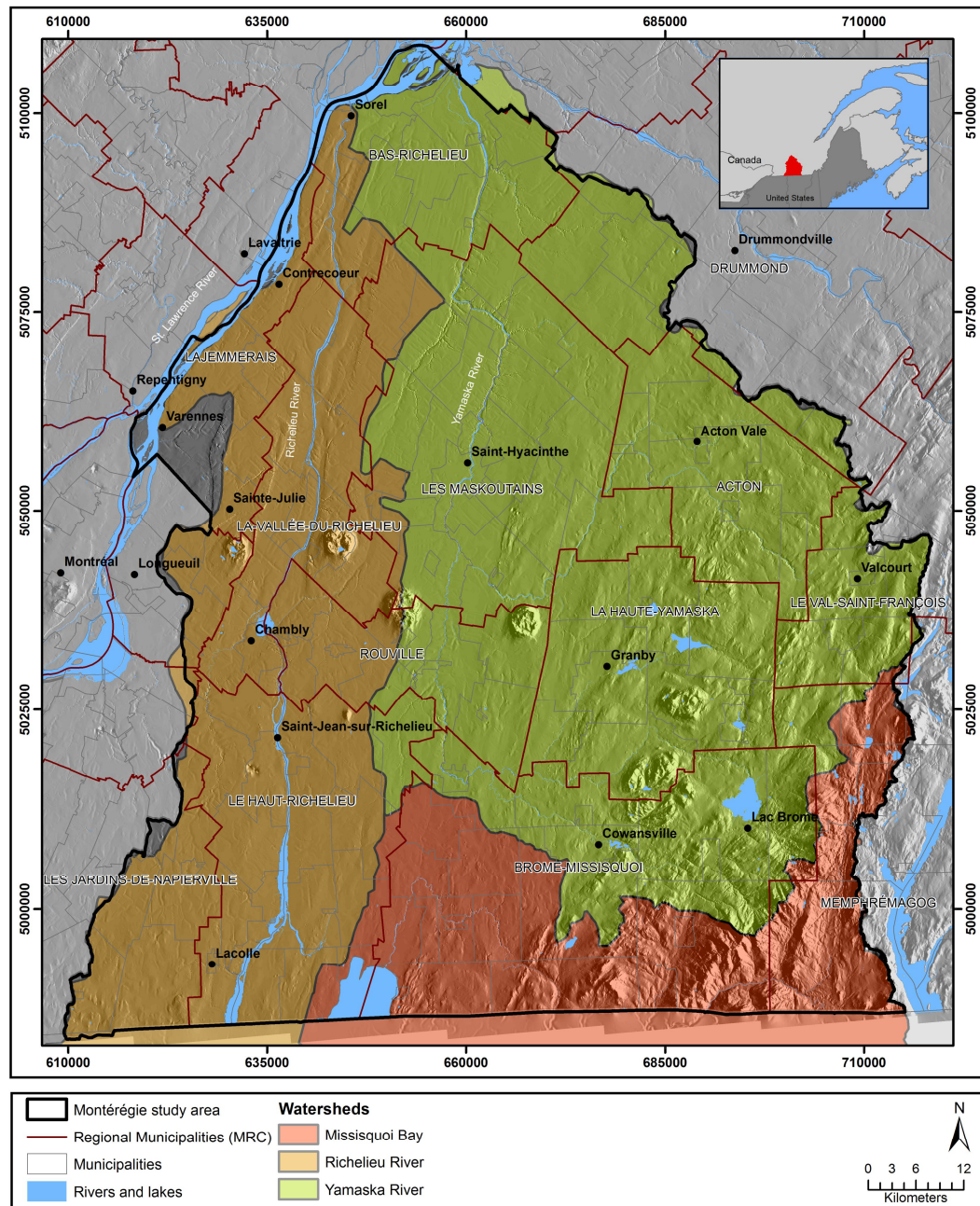


Figure 1 : Location of the study area, east of Montreal in southern Québec (Montérégie Est), showing the boundaries of regional municipalities (MRC) and the main cities.

1.1.2 Geological contexts in the study area

The Canadian portion of the study area includes three geological contexts defined by the regional geology: the St. Lawrence Platform, the Appalachians, and the late-stage intrusives corresponding to alkaline granitoid intrusives of the Monteregian Hills and dioritic intrusives (Figure 2).

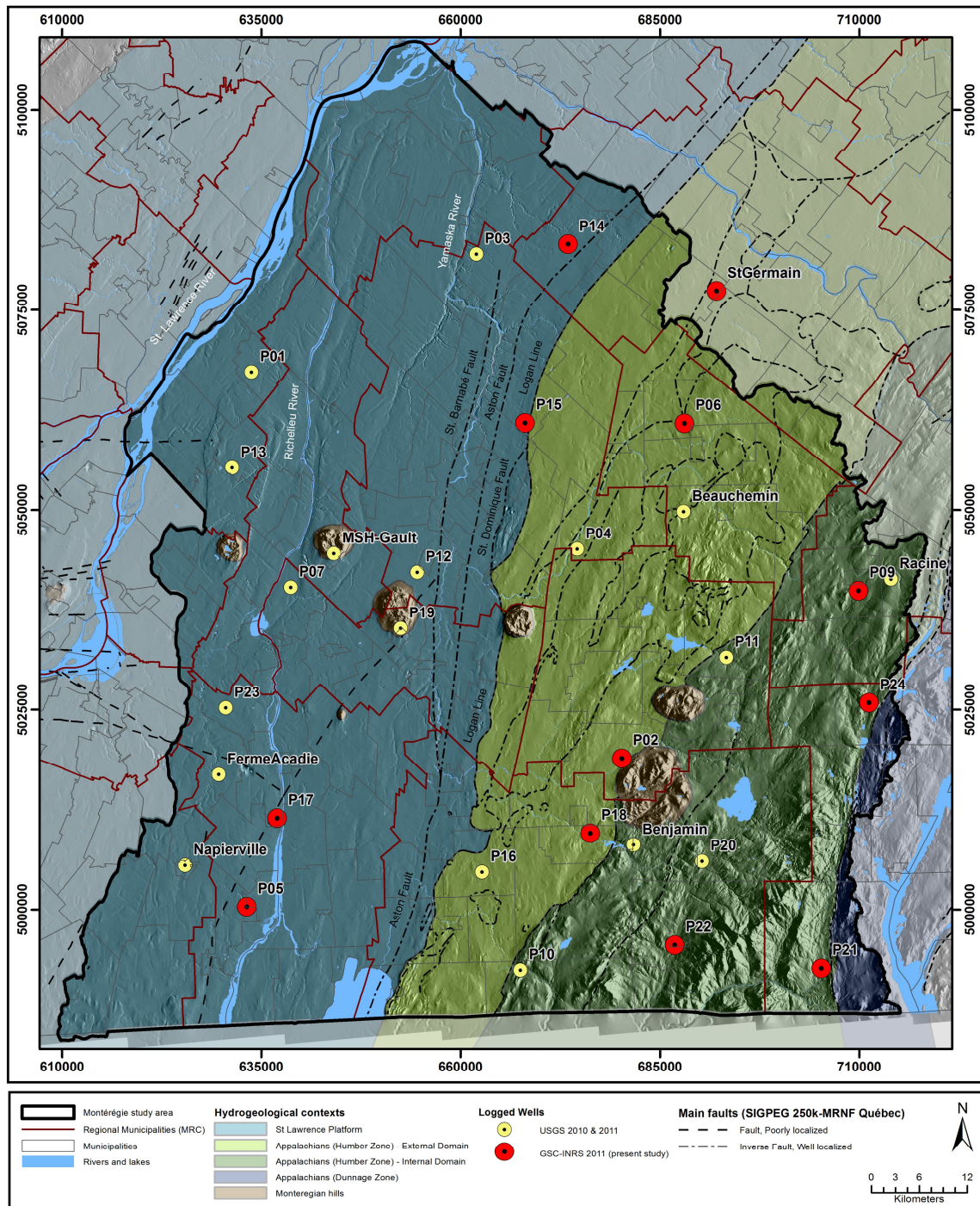


Figure 2. Hydrogeological contexts of the Montérégie Est area and borehole locations

The St. Lawrence Platform is located in the western part of the study area, from the St. Lawrence River to the Logan Line to the east. The eastern limit of the St. Lawrence Platform corresponds to an imbricate fault zone (including the St. Barnabé, Aston, and St. Dominique faults) of which the Logan

Line is the easternmost fault (Globensky, 1987). In the St. Lawrence Platform, limestone and shale lithologies are dominant, with subordinate sandstones and dolomites. Rock units were little deformed by the Chambly-Fortierville syncline (Globensky, 1987).

The Appalachian rocks in this study area include two zones on the Canadian side: the Humber zone, which occupies most of this area, and the Dunnage zone, which corresponds to a small band on the eastern side. The Humber zone is mainly composed of Cambrian-Ordovician sedimentary clastic rocks but also includes some volcanics, while the Dunnage zone is mainly composed of volcanics, but also contains ophiolites and sedimentary clastic rocks of Ordovician age (Williams, 1979). The Humber zone can be divided into two sub-zones roughly equivalent to the Appalachians internal and external domains as defined in Slivitzky and St-Julien (1987). Differences between these two domains mainly reside in their degrees of metamorphism and deformation, which are more intense in the uplands (internal domain). Sedimentary rocks of these two zones are composed of varied assemblages of shales of different colors, green sandstones, clayey limestones, and dolomites. These Appalachian rocks were mainly deformed during the Ordovician Taconian Orogeny, then, to a lesser extent, structurally re-activated during the Middle Devonian Acadian Orogeny.

1.1.3 Previous downhole geophysical surveys

In 2010, eighteen open-rock boreholes (PO-series) were drilled as part of the GSC-INRS Phase I drilling program in the Montérégie Est area (Figure 2). These boreholes, and an additional six existing municipal wells, were logged by members of the United States Geological Survey (USGS) during three field trips carried out in October and November of 2010, and June 2011. Logs collected included three-arm caliper, natural gamma, fluid temperature and fluid resistivity, near (16”) and far (64”) normal resistivity, full waveform sonic, flowmeter, and acoustic televiewer (ATV), using instruments manufactured by Century Geophysical Corporation. These data were available for review by the authors, but have not been published at this time.

In 2011, an additional four boreholes were drilled (PO-02, -14, -18, -22) as part of the Phase II drilling program, requiring a final field trip to complete the geophysical surveys. As the USGS researcher had retired over the summer of 2011, a geophysicist from the GSC office in Ottawa (H. Crow) completed the logging in October 2011 with INRS graduate students (M. Laurencelle and P. Ladèveze). During this field trip, the four new holes were logged with a full suite of tools (natural gamma, apparent conductivity, magnetic susceptibility, fluid temperature, heat-pulse flowmeter, and acoustic televiewer), and eight of the Phase I holes were re-logged with a subset of this suite. This report focuses only on the twelve boreholes logged during the GSC field trip in October 2011, but does present some of the USGS data from the eight re-logged wells.

1.1.4 Borehole site selection

Borehole locations for the drilling program (Phases I & II) were selected to adequately cover the study area’s different geological formations and hydrogeological regimes, and fill knowledge gaps in stratigraphy, geochemistry, or hydraulic properties. Drill sites were chosen based on available water-well data from the “Système d’Information Hydrogéologique” (SIH, managed by the MDDEFP), geological maps and cross-sections, as well as data acquired during the 2010 and 2011 field campaigns (including piezocone surveys and preliminary seismic reflection results). Equally important was the selection of sites where boreholes could be easily reaccessed for future testing. Table 1 lists basic information for the wells logged during the GSC campaign.

In addition to the shallow bedrock wells of Phases I & II, deeper municipal wells were targeted to gain knowledge of groundwater circulation at greater depths (generally > 50 m). Unfortunately, very few municipal wells are idle and only one could be accessed for this study.

Table 1. Basic borehole information for the logged wells.

Borehole ID	Municipality (QC)	Drilling Method	Drilling Date	Depth to Bedrock (m)	Borehole Depth (m)	Most Recent Water Level (m; date)
PO-02	Bromont	Rotary	2011-10-03	20	37	1.5 (2011-10-31)
PO-05	Saint-Paul-de-l'Île-aux-Noix	Rotary	2010-10-18	11	24	1.2 (2011-10-26)
PO-06	Saint-Théodore-d'Acton	Rotary	2010-10-05	3	55	1.6 (2011-10-24)
PO-09	Valcourt	Rotary	2010-11-03	6	22.5	1.9 (2011-10-24)
PO-14	Saint-Guillaume	Rotary	2011-10-04	28	43	5.0 (2011-10-27)
PO-15	Saint-Simon	Rotary	2010-11-10	11	29	3.2 (2011-10-24)
PO-17	Saint-Jean-sur-Richelieu	Rotary	2010-11-09	21	36	3.1 (2011-10-26)
PO-18	Cowansville	Rotary	2011-09-30	41	57	10.4 (2011-10-25)
PO-21	Potton	Rotary	2010-11-05	23	40	18.4 (2011-10-25)
PO-22	Sutton	Rotary	2011-09-28	28	49	0.3 (2011-10-25)
PO-24	Eastman	Rotary	2010-10-21	16	30	0.7 (2011-10-24)
St-Germain (#26)	Saint-Germain-de-Grantham	N/A	N/A	10	146	28.29 (2011-10-18)

2.0 Fieldwork

2.1 Drilling methods and sample collection

Drilling operations were supervised by personnel of INRS-ETE or the GSC. The Phase I boreholes were completed in 2010 by Groupe Puitbec from Victoriaville, QC, using a dual rotary drill rig (Foremost model DR-12, see Figure 3). The second phase of drilling in 2011 was completed by A & G Puisatiers Experts from Granby, QC, with a standard rotary drill (Driltech model T25K4W) and an Odex casing system (see Figure 4).

All the PO-series wells were drilled with a 150 mm (6") diameter bit and encountered bedrock at a minimum depth of 13 m. Samples were retrieved at regular intervals from the drill cuttings for basic geological descriptions. Upon completion, the wells were flushed by circulating fresh water to the base of the borehole until the water ran clear at the ground surface, taking 20 to 60 minutes.

The boreholes were sampled for conventional geochemistry, and underwent slug testing to obtain hydraulic conductivity (K). Following geophysical logging, they became observation wells that were integrated in the provincial monitoring network of the MDDEFP.



Figure 3. Dual rotary drill rig (Foremost model DR-12) used for Phase I drilling in 2010.

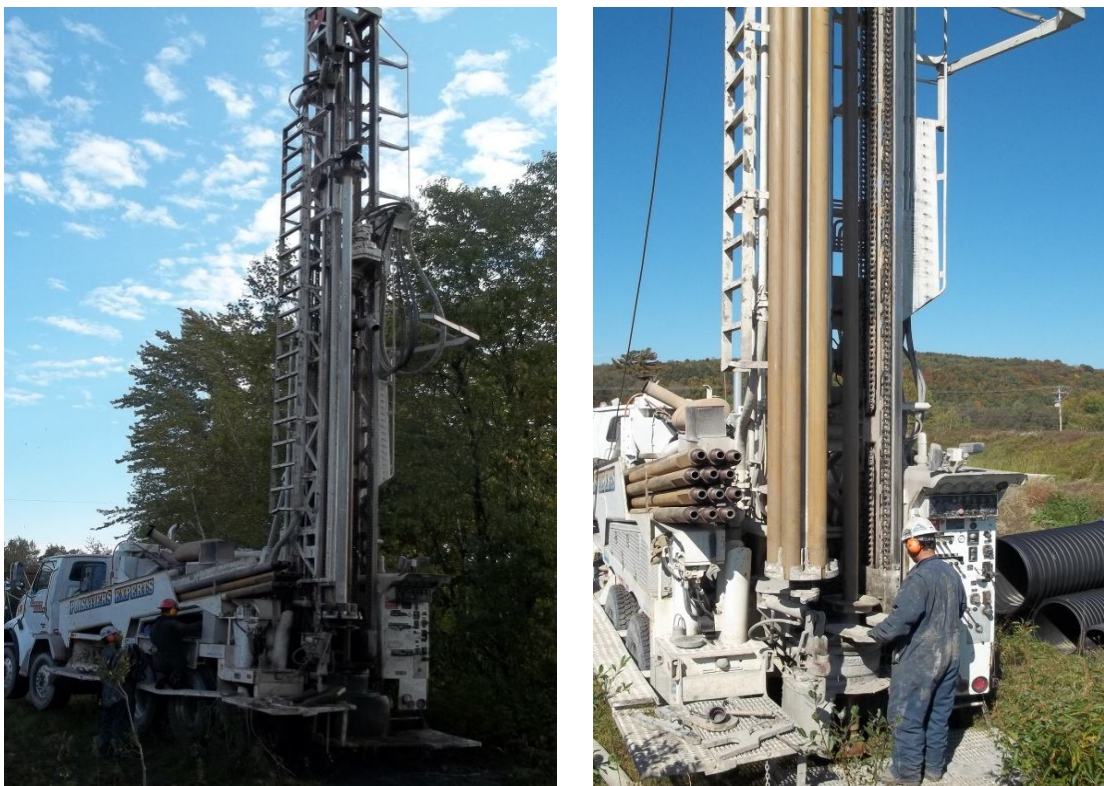


Figure 4. Standard rotary drill rig with Odex system (Driltech model T25K4W) used for Phase II drilling in 2011.

2.2 Geophysical logging

Fieldwork was carried out between October 12th and 20th, 2011. Table 2 contains a summary of the logs collected in each borehole, and Table 3 describes the logging tools' units, data resolution, logging details, and the practical interpretation of each log. More detailed information on each tool can be found in Appendix I. In the eight re-logged boreholes, the acoustic televiewer (ATV) and magnetic susceptibility tools were run, and if the hole appeared to be hydraulically conductive from the USGS tests, the temperature and heat pulse flowmeter were also run.

Geophysical logs provide a means of identifying and characterizing lithological units based on variations in their chemical and physical properties. "Lithological logs" (spectral gamma, conductivity, magnetic susceptibility) augment geological interpretation when samples cannot be retrieved, and permit fine tuning of geological contact depths when cuttings are collected at the surface. The group of logs known as "hydrogeophysical" (fluid temperature, flowmeter, caliper) permit the detection of fluid movement within the open wellbore, or even behind the casing (temperature only), allowing for the inference of groundwater movement and flowing fractures. Finally, the ATV collects high-resolution images, in amplitude and time, of the inside of the borehole wall. This allows for analysis of the wall roughness, orientation of structural features (strike direction, dip), and estimation of the fracture aperture at the borehole wall. The televiewer log can be considered structural, hydrogeophysical, and to a lesser extent, lithological, in groundwater studies.

Table 2. Geophysical logs collected during the logging field trip in October 2011.

ATV= acoustic televiewer, HPFM=heat pulse flowmeter.

Borehole	Drilling Phase	Geophysical Logs					
		Structural	Hydrogeophysical		Lithological		
		ATV & caliper	HPFM	Temp.	Magnetic Suscept.	Spectral Gamma	Apparent Conductivity
PO-02	II	✓	✓	✓	✓	✓	✓
PO-14	II	✓	✓	✓	✓	✓	✓
PO-18	II	✓	✓	✓	✓	✓	✓
PO-22	II	✓	✓	✓	✓	✓	✓
PO-05	I	✓		✓			
PO-06	I	✓			✓		
PO-09	I	✓	✓		✓		
PO-15	I	✓			✓		
PO-17	I	✓	✓		✓		
PO-21	I	✓			✓		
PO-24	I	✓			✓		
St-Germain	-	✓					

Table 3. Summary of the downhole log suite, including logging unit, data resolution, logging details, and practical interpretations of each log.

Downhole Geophysical Log <i>[Manufacturer]</i>	Logging Unit	Radius of Investigation <i>[Vertical resolution]</i>	Logging Speed	Logging Interval	Practical interpretations in open rock
Spectral Gamma <i>[Mount Sopris]</i>	Counts per second (cps)	0.3 - 0.6 m <i>[centimetres, function of logging speed]</i>	1 m/min	0.01 m	Relative grain-size, lithological boundaries
Apparent Conductivity <i>[Geonics/Mount Sopris]</i>	milliSiemens /meter (mS/m)	0.3 m <i>[submetre]</i>	3 m/min	0.02 m	Formation conductivity (grain and/or porewater conductivity), lithological boundaries
Magnetic Susceptibility <i>[Geonics/Mount Sopris]</i>	parts per thousand SI (ppt SI)	0.3 m <i>[submetre]</i>	3 m/min	0.02 m	Magnetite (heavy mineral) concentration, lithological boundaries
Temperature <i>[GSC]</i>	Frequency, converted to degrees Celcius (°C)	Influenced by surrounding materials <i>[logging interval]</i>	1 m/min	0.01 m	Anomalies due to groundwater flow; lithology (as related to thermal conductivity)
Heat Pulse Flowmeter <i>[Mount Sopris]</i>	US Gal/min	Within borehole 0.03 USGal/min	Stationary readings	User selected; based on ATV and fluid temp. results	Direction and volume of flow, zones of hydraulic conductivity
Acoustic Televiwer <i>[Advanced Logic Technology/ Mount Sopris]</i>	Dual images: Traveltime (millisec) Amplitude (unitless)	Open face of borehole wall Minimum azimuthal resolution: 1.25 pixel/deg <i>[Minimum scan width: 0.001 m]</i>	0.5 m/min	0.001 m	In open rock: structural orientation (strike direction & dip), fracture aperture at borehole wall
Acoustic Caliper Interpreted from ATV traveltime data	mm	Open face of borehole wall [Caliper resolution: 0.0001 m]	0.5 m/min	0.001 m	Wall roughness, fracture aperture at borehole wall

Laboratory calibrations were performed with the temperature tool, flowmeter, and orientation systems of the ATV tool before leaving for the field.

Upon arriving at a well site, the downhole water level was measured using a water level meter. Geophysical data were then acquired using a Mount Sopris logging system with a Matrix console and interchangeable downhole probes, with the exception of the temperature tool. A laptop computer recorded the data using the Matrix logging software. The temperature log was collected with the in-house GSC temperature tool coupled with a Geonics winch and GSC logging software. On site calibrations were carried out with the conductivity and magnetic susceptibility tools before the logging runs. Corrections for sensor offset and casing stick up for all tools were made prior to logging, and logs were recorded relative to ground surface.

The temperature tool was always the first instrument lowered into the borehole to avoid disturbing the borehole fluid. A period of 15-30 minutes was allowed for the tool to thermally equilibrate in the top of the water column before the logging was started. Gamma, conductivity, and magnetic susceptibility were then collected in any order, followed by the televiwer. Once the televiwer and temperature logs were reviewed together, intervals for the heat pulse flowmeter testing were selected to bracket visible deviations in the temperature log, and/or presence of open (or partially open) fractures seen in the ATV images.

The acoustic televiwer was centralized in the borehole using a pair of aluminum, four-arm, bowspring centralizers. As decentralization negatively affects the quality of the image, care was taken to ensure the tool was well centered in the borehole before the log was recorded. Due to the large borehole radius (~150 mm diameter), the maximum resolution was used for the logging (288 pts per revolution, or 1.25 pixels/deg, with 0.001 m logging intervals). The logs were always collected from the bottom of the hole upwards, to keep constant tension on the wireline at low logging speeds.

During heat pulse flowmeter testing, ambient flows (i.e. natural upward/downward gradients in borehole fluid) were not observed in any of the boreholes. Therefore, a Redi-Flo 2 Grundfos pump and controller unit were used to induce upward flow in the borehole. The pump could be lowered to a maximum depth of 25 m, which would ideally place it within the bedrock. However, since surficial sediments were frequently thicker than 25 m, the pump often had to be left inside the casing. Flow rate was monitored every few minutes on surface using a graded bucket and a stopwatch, while water levels were measured in the borehole using a water-level meter. The flow rate was carefully adjusted to not exceed the tool's upper limit of 1.0 USGal/min (3.78 L/min), and also to equalize the pumping rate with the recharge (i.e. no measurable drop in water level during the pumping). In practice, this was difficult to achieve, as many of the boreholes did not intersect highly permeable fractures.

To ensure the change in flow rate measured by the tool could be attributed to changes in hydraulic conductivity and not to changes in the pumping rate, achieving a constant rate was a very important element of the test. In non-hydraulically conductive boreholes, reaching stability is very difficult, and was sometimes not possible. This occurred in PO-18, and the flow results were therefore converted from a volumetric value, to a percentage of the total pumping rate measured simultaneously at the surface during the downhole flow measurement.

Once the pumping levels were stabilized (in all but PO-18) which could take up to 45 minutes, the test began with the tool positioned at the first depth of interest. Once three heat pulse triggers yielded the same values (± 0.02 USGal/min), the test continued, moving the tool to the next target depth. Five-to-ten minutes were given for the fluid to stabilize after the tool was moved in the borehole. The logging

concluded with a final test inside the casing to indentify whether the contact between casing and bedrock was sealed.

3.0 Data Analyses

3.1 Log data

Downhole log data were imported into WellCAD processing software and displayed in a composite figure for each borehole. Each figure contains an interpretation column displaying depths of lithological boundaries and geophysical observations, based on a review of the entire log suite (see Appendix II). Flowmeter results are summarized in Appendix III. Samples of the structural classes developed for this project are shown in Appendix IV. Logs were also exported from WellCAD in digital form (see Appendix V).

In cases where Phase I boreholes were re-logged, USGS resistivity logs, full waveform sonic velocities, and occasionally temperature and heat-pulse flowmeter logs, are incorporated into the figure. The resistivity data essentially act as a lithological log (resistivity is the inverse of conductivity), and sonic velocities act as an indicator of bedrock hardness.

3.1.1 Lithological logs

Total count (TC) spectral gamma data were converted to weight percent potassium (K), uranium (U), and thorium (Th) using calibration curves developed at the USGS calibration facility in Denver, Colorado. Due to the very low number of counts in each of these energy windows (generally 4 or less), the values were not considered statistically significant, and data are therefore only displayed as TC. Variations in the natural gamma logs are readily visible within the bedrock (and even within the cased overburden materials) identifying numerous changes in bedrock and overburden lithology.

Electromagnetic induction logs (conductivity and magnetic susceptibility) were cut off within the metal casing where they do not collect meaningful data, but were otherwise unaltered. The responses, when interpreted with the gamma log, were very effective in identifying variation in lithology, particularly when bedrock changed from one type to another (e.g. PO-02, PO-18, St-Germain). Even in cases where the geological log describes the rock as one type in the, small changes in the lithological log suite can be observed (e.g. PO-09, PO-21, PO-22, PO-24) indicating interbeds of another rock type, or variation in the chemical properties of the rock. These changes also have the potential to represent zones where physical weaknesses could develop along contact zones, leading preferential pathways for fluid flow.

3.1.2 Hydrogeophysical logs

The temperature log was run using GSC software which converts a frequency measurement to temperature, and also computes the gradient (dT/dz , °C/m) to assist in identifying zones where fluctuations occur over very small changes in temperature. The GSC temperature tool measured groundwater temperatures ranging from 7.70 to 9.80°C in the bedrock, with most ranging between 8.00°C and 9.00°C. In general, the temperature logs did not reveal many significant temperature gradient anomalies in the bedrock corresponding to temperature changes greater than 0.1°C. However,

when observed, these locations coincided with fractures in the ATV image and zones of flow under pumped conditions with the heat pulse flowmeter (e.g. PO-14, 30 m depth). They could also coincide with changes in temperature behind the casing wall where fluid flow in the overburden material influenced the temperature of the fluid inside the casing. This was particularly noticeable at the overburden/bedrock boundary in PO-09.

Heat pulse flowmeter results are presented in bar chart form in Appendix II, and in detailed tables in Appendix III. The tests did not indicate any detectable natural flow in the boreholes logged. In general, the boreholes did not contain many hydraulically conductive fractures, except in boreholes PO-02, PO-09, PO-17, and St-Germain where flow was measured under artificial (pumped) conditions. In a few cases, (e.g. PO-14, PO-18), flow was measured at the casing/bedrock interface, suggesting a poor casing seal allowing groundwater to flow in from the overburden/bedrock contact. Due to the low flow levels in these boreholes, the heat-pulse flow meter is an appropriate choice, as it is capable of detecting natural and pumped flow at levels as low as 0.03 USGal/min (0.11 L/min).






3.1.3 Structural logs

Acoustic televiewer files were imported into the WellCAD image processing module, and traveltime and amplitude images were immediately oriented to magnetic north. The data range and color palate of the two images could be adjusted to improve the on-screen resolution of the structural features. The ATV data appear in the software as an unwrapped image of the inside of the borehole wall, making any dipping structures look sinusoidal.

Before interpreting the images for structural orientation, the borehole diameter must be accurately known, as this value influences the dip of the interpreted structural features. Therefore, a caliper log was calculated using the 360° traveltime data collected during the ATV logging run. As the drilling method used a downhole hammer, the borehole walls could be quite rough, resulting in lost or attenuated acoustic signal in cavities, rough walls, or open fractures. When the signal is lost, the only acoustic reflector detected by the tool is the first multiple of the reflected acoustic signal on the tool's acoustic window. This creates an early arrival time which interferes with the caliper calculation: therefore, these times were removed from the traveltime dataset using a filter. The diameter was then calculated using an assumed fluid velocity of 1427 m/s, which takes into account the temperature of the water based on the fluid temperature logs, and assumes the water is clear: a reasonable assumption, given the quality of the water drawn from the well during the pumping tests. From these traveltimes, the software calculates minimum, maximum, and average borehole diameters, which were compared with the known diameter of the casing for verification. Having the three computed caliper logs (min, max, & average) enhances the interpretation of structural features, as a continuously open fracture will increase in diameter in both the minimum and maximum logs.

A structural column was created and linked to the “average” caliper log. A structural classification system was created to categorize the feature types of interest in the project (shown in Table 4). Features which are open are those which could transmit groundwater, and those which are closed are indicative of structural features in the region (joint sets, bedding orientation, foliation, etc.). A broken zone is distinguished from an open feature by being continuously fractured over more than a vertical distance of 0.5 m, coupled with an increase in borehole diameter of greater than 25 mm beyond the nominal diameter. Broken zones may be caused by intersecting fractures or zones of weakness. Appendix IV contains sample images of these structural categories from the wells.

Table 4. Acoustic televiewer structural classification for the Montérégie Est characterization project.

Structure Type	Structure Sub-type	Sample Structure	Structure Code
Broken Zone	-	Intersecting fractures, weakened zone	BZ 
Open Feature	Continuous fracture with aperture	Open joint, bedding partings	OC 
	Discontinuous fracture with aperture	Partially open joint, bedding partings	OP 
Closed Feature	Parallel	Low angle bedding, foliation	Cpl 
	Perpendicular	High angle joints	Cpr 

Once sinusoids were fit to the structures, they were classified according to Table 4 and then exported relative to magnetic north and corrected for borehole tilt. Data were subsequently corrected for declination for stereogram presentation by INRS-ETE, using NOAA's "Estimated Value of Magnetic Declination" [online](#) calculator at each well location.

3.2 Structural data

3.2.1 Methodology

Table 4 presents the classification scheme used during the structural analyses of televiewer images. Planar structural features were plotted as points on stereograms, representing feature poles after plane projection on the lower hemisphere of an equal-area Schmidt diagram. Feature density plots based on orientation were then computed. The objective of this structural analysis was to research the orientation of fracture sets which are potential flow pathways. The analysis of the orientation data was carried out using Stereo32 software package version 1.0.3 (Roller and Trepmann, 2011).

As logs were recorded in vertical boreholes, there is an unavoidable under-sampling of the structures that are subparallel to the borehole axis, leading to an orientation bias. This causes an underestimation of subvertical features, an effect which has been observed and discussed by many authors (Baecher, 1983; Kulatilake and Wu, 1984; Park and West, 2002). Consequently, a weighting factor was applied to each orientation measurement to compute a more representative proxy of the real number of intersecting fractures for the various orientations. This method is known as "Terzaghi correction" (Terzaghi, 1965), and is discussed more recently by Priest (1993). This weighting factor, w , is calculated using the angle between the sample line (i.e. the near-vertical axis of the borehole) and the dip of the sampled planar feature:

$$w = \frac{1}{\cos(dip)} \quad (\text{Eq. 1})$$

Because of the technical limitations of the Stereo32 software, each feature had to be plotted [10·w] times in the density stereogram to take this weighting factor into account.

However, the general disadvantage of the Terzaghi correction is that the number of very steeply dipping features will be overestimated (Terzaghi, 1965). To avoid this new source of error, Terzaghi proposed to sample cores from boreholes oriented in various directions and dip angles. The steeply dipping planar features with angles nearly parallel to the borehole axis fall within a range coined by Terzaghi (1965) as the “blind zone”. The size of the blind zone is discussed by authors such as Goodman (1976), and more recently, by Roy et al. (2011) who recommends using a blind zone of 20°. In our study, most holes are nearly vertical, having a deviation ranging from 0° to 5°, with two wells (PO-06 and St. Germain) having deviations reaching 10°. To limit the introduction of errors from steeply dipping features, structures which fall into a blind zone of 20° (structures dipping 70° or more) were given a weighting factor of zero.

3.2.2 Results

Interpretation of structural data was carried out using Figures 5 through 7. Figure 5 shows the number of features for each structure type and geological context. Figure 6 presents stereograms for the 12 boreholes, also grouped by hydrogeological context. Figure 7 presents the stereograms and contoured pole-density diagrams — with both uncorrected and corrected orientations following the Terzaghi approach — for all data, and then for open features only. This allows for analysis of open-feature-specific orientations and possible identification of preferential flowpath trends. Note that broken zones are excluded from these orientation analyses as their dips are undefined.

Feature type ratios in each hydrogeological context:

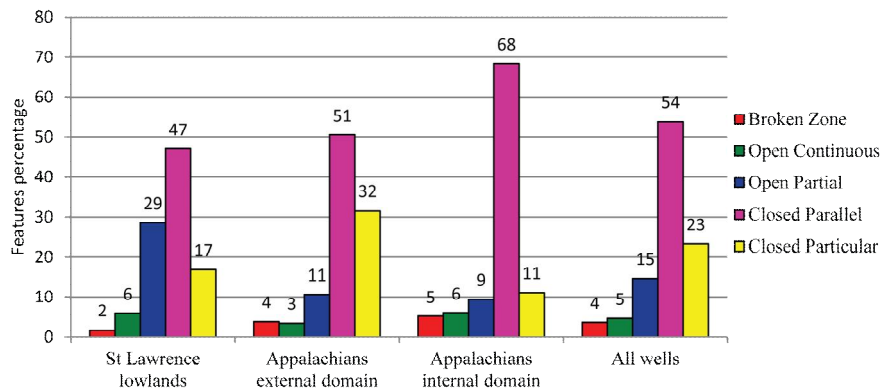


Figure 5: Percentage of features observed in the logged wells, by type and hydrogeological context.

Figure 5 shows that observed feature count by type is unequal. Presence of closed parallel (shallow dipping) features (54%) is ubiquitous whereas all open features make up a much smaller subset of the data. Thus, it is important to distinguish between open and closed features when looking at structural data or plots, since only open features have the potential to be water-bearing fractures, supposing that the defined open-vs.-closed threshold is a good proxy for the real hydraulic behaviour of those fractures.

Feature orientations for each well

Figure 6 (a, b, c) shows stereograms (without Terzaghi corrections) for the observed features in each well, grouped by hydrogeological context.

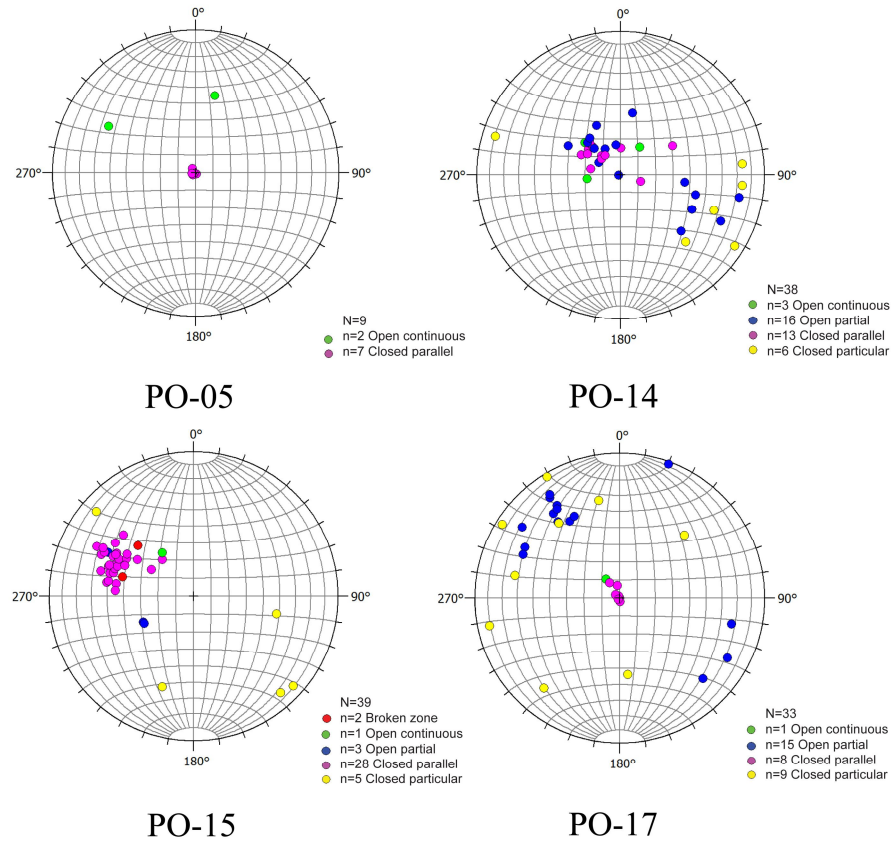


Figure 6a: By-well stereograms for boreholes in the St. Lawrence Platform (Equal area projection in the lower hemisphere).

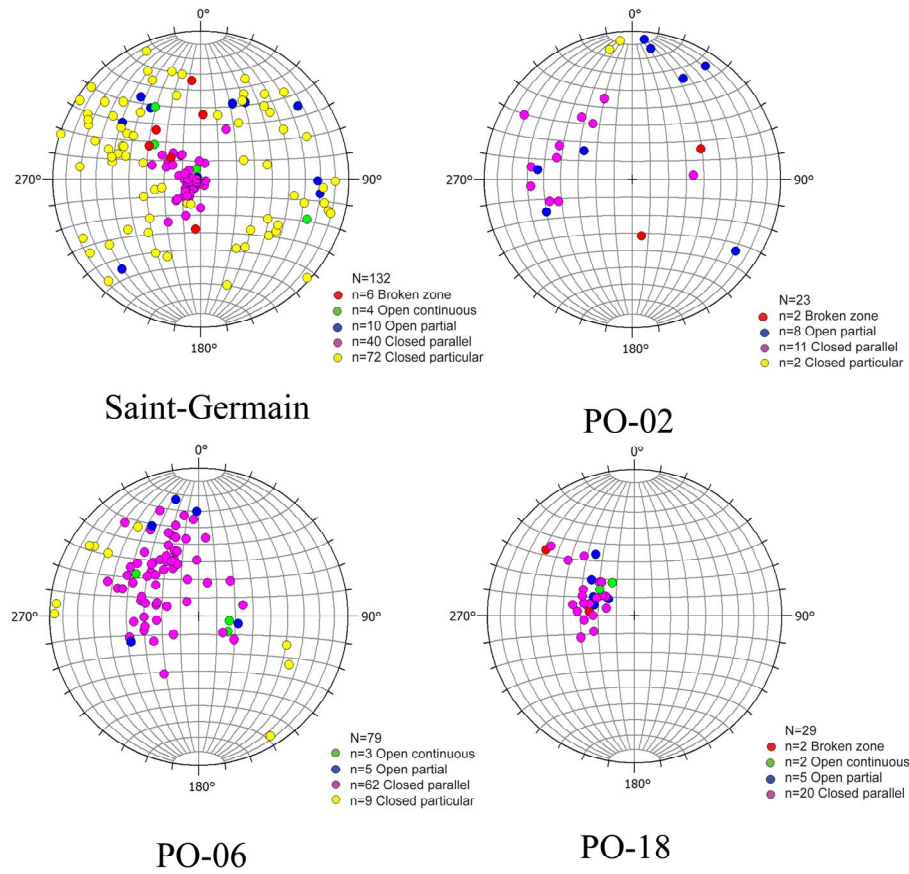


Figure 6b: By-well stereograms for boreholes in the Appalachians external domain (Equal area projection in the lower hemisphere).

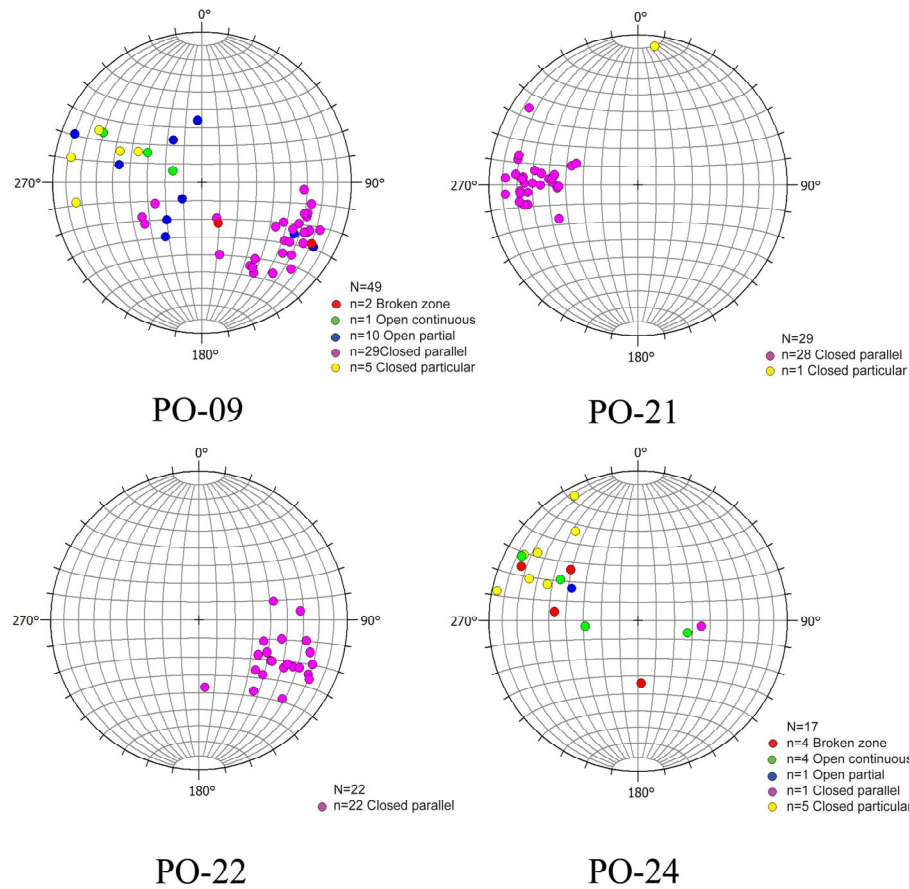


Figure 6c: By-well stereograms for boreholes in the Appalachians internal domain (Equal area projection in the lower hemisphere).

Closed features

A comparison of all the stereograms shows that the greatest distribution of structural orientations is observed in the St-Germain and PO-06 wells. In all of the wells, the closed-particular features do not show any preferential orientation.

Clear clustering of closed-parallel feature orientations is observed in Figures 6a, b, & c, especially in PO-15, PO-17, PO-18, St-G., PO-21, and PO-22. Closed-parallel features dipping $< 10^\circ$ are observed in wells PO-05, PO-17, and St-Germain. In the other wells, features of this type share a common strike, roughly N 45° , though dipping either north-west (PO-09, PO-22) or south-east (PO-06, PO-15, PO-18, and PO-21) with plunge angles ranging between 25° and 60° .

Open features and aperture interpretation

The orientations of open-continuous features fall within the ranges of the open-discontinuous features. However, open-continuous features do not show a clear clustering in any stereogram when viewed on a by-well basis. Very few open features are shallow-dipping (i.e. subhorizontal).

When a planar fracture intersects the borehole at some angle to the well's axis, one can expect an increase in the apparent aperture of the fracture in the image. As the increase factor equals $(\cos \Theta)^{-1}$, an open feature with a high dip of 65° , for example, could appear 2.4 times wider at the maximum and

minimum of the sinusoid than a horizontal feature. (Note that this aperture bias differs from the sampling bias that is corrected using Terzaghi's approach, though the factor is identical.) In addition, the drilling process (particularly the hammer method) tends to increase the fracture aperture at the borehole wall. Therefore, interpretation of aperture from borehole wall images can overestimate the aperture of fractures extending back into the rockmass.

Feature orientations for the whole study area

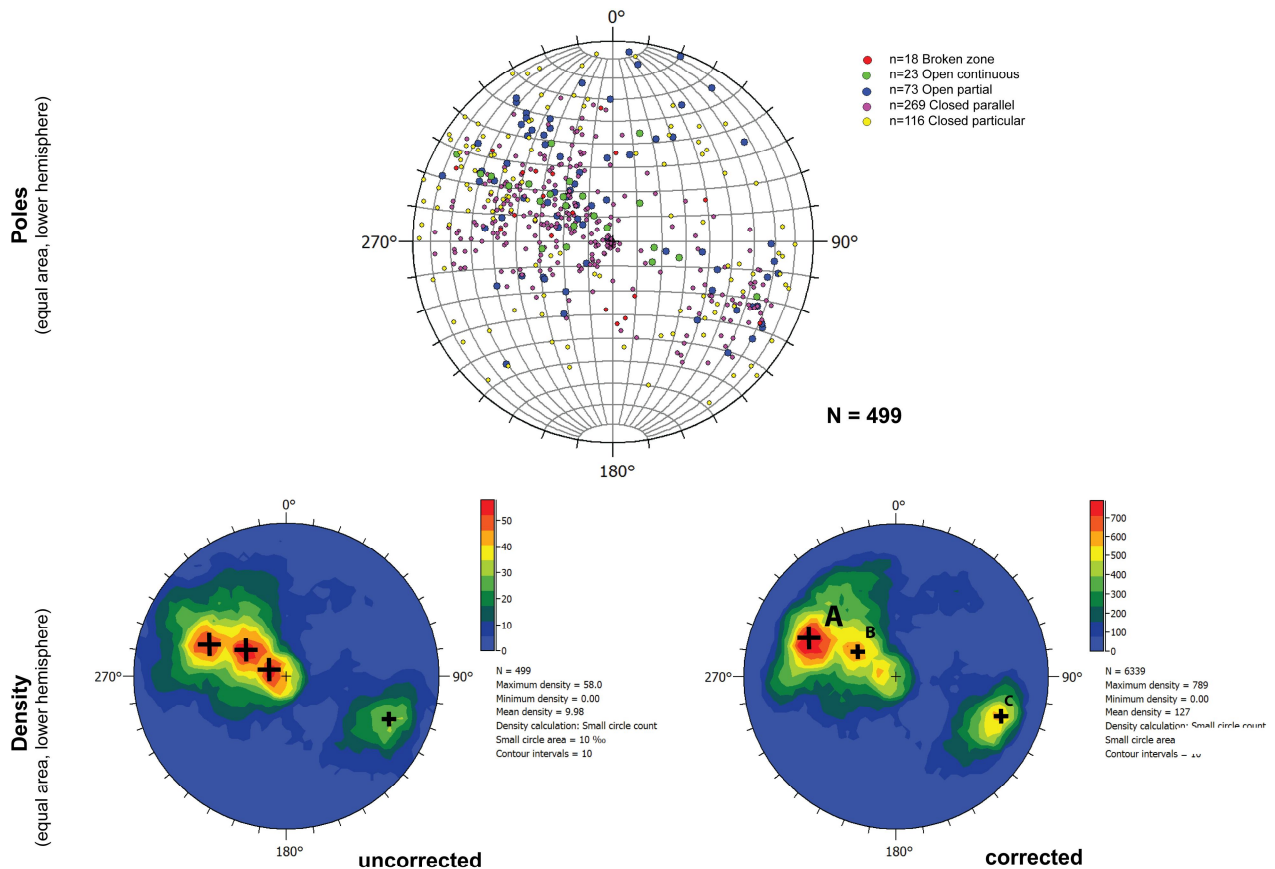


Figure 7a: Stereograms and contoured pole-density plots using all features gathered for all wells (before and after applying Terzaghi correction). Crosses A, B, and C define structural feature sets.

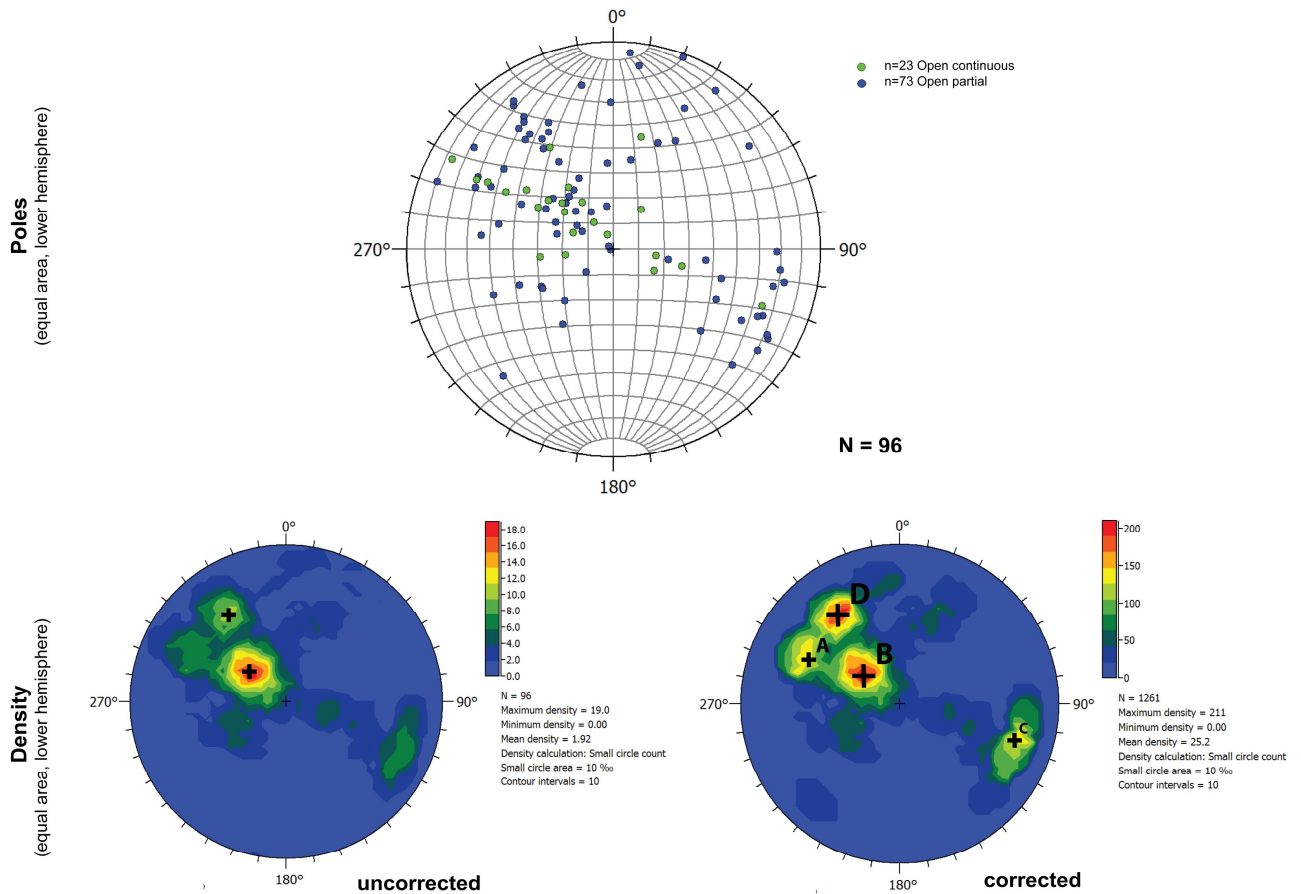


Figure 7b: Stereograms and contoured pole-density plots of open features (open continuous and open partial, n=96) from all wells (before and after applying Terzaghi correction). Crosses A, B, C, and D define structural feature sets.

Table 5: Average orientations (relative to geographic north) for the four structural sets identified in the study area.

Set	Strike direction (°)	Dip direction (°)	Dip angle (°)
A	31 (NNE-SSW)	121 (ESE)	56
B	38 (NNE-SSW)	128 (ESE)	23
C	16 (NNE-SSW)	286 (WNW)	68
D	57(ENE-WSW)	147 (SSE)	57

In Figures 7a and 7b, up to four structural feature sets (labeled A, B, C and D) are identified using the Terzaghi-corrected density diagrams. Table 5 summarises the mean orientation for each set. The pole diagrams and the uncorrected density diagrams are shown for comparison.

With the all-feature corrected density plot, the major set appears to be A (Figure 7a). The four sets are distinguished simultaneously only when examining the open features (Figure 7b). Among the open features, two main sets can be distinguished: B and D. But given the limited number of open features, the assumption of a unique set gathering A, B and D sets can be made.

3.2.3 Discussion

In this section, initial interpretations for the structural data are proposed, focusing on results presented in Figures 5, 6, and 7. Additional work will be carried out to better understand the significance of these results on the regional groundwater system (see section 5 on future research).

Distinction between “closed” and “open” features gives insight into both stratigraphic and structural details of the rock setting, and especially on potential preferential pathways for groundwater. Using the flowmeter results, open features can be further classified as “permeable”.

The most frequent features interpreted in the televiewer images were closed parallel and perpendicular structures totalling 77% of all observed features (Figure 5), while broken zones represent 4%, and open/partially open features, 20%. Analysis of interpreted structural log data does not show a clear open-feature pattern when boreholes are analysed individually (Figures 6a, b, c). Two wells (St-Germain and PO-06) show a wide scattering of their feature orientations, which could be related to a strong intrinsic heterogeneity of the local geological formation.

In the well-by-well analysis, closed parallel (CPI) features are generally interpreted as bedding features. In the St. Lawrence Platform context, the bedding planes are subhorizontal, since rocks are gently deformed. PO-15 is the only well in this context that does not share this trend (high-dipping CPI features are observed), likely because it is located close to a fault area where bedding planes are folded. In the Appalachians context, closed parallel features are dipping at various angles, which may be due to the folding induced by the thrust-sheet systems developed during the compressive period of the Appalachian orogeny. Most of the features observed in the wells are compatible with a NNE to NE common strike direction (Figure 6, Table 5).

Processing of the structural data using stereograms revealed four orientation sets. The four fracture sets share a NNE to NE common strike direction (Figures 7a & b, Table 5). This strike direction is aligned with dominant faults and folds axes of the St. Lawrence Platform and Appalachians contexts (Clark, 1964a; Clark, 1964b; Faure, 1995; Faure et al., 2004; Globensky, 1987; Rocher et al., 2003; Slivitzky and St-Julien, 1987).

Sets A, B and D have relatively similar orientations, so that they might correspond to only one set with some scatter. Overall, sets A, B and D are dipping SE, while set C is dipping NW. In other words, set C is oriented perpendicular to A, B, and D. As most closed-parallel features are clustered in sets A, B and D, it is theorized that bedding planes are dipping 25°-60° toward the SE. Results of this preliminary structural interpretation indicate that open fractures sets are roughly parallel to bedding planes (sets A, B and D) with an orthogonal set roughly perpendicular to the bedding planes (set C). Orthogonal fracture sets are quite likely in hard, layered, sedimentary rocks with long-wavelength folds.

4.0 Conclusions & Recommendations

4.1 Influence of the drilling method and borehole depth on structural dataset

There was not a significant difference in wall roughness, and thus televiewer image quality, between the DTH hammer and Odex methods used in drilling Phases I and II. Wall roughness was seen to depend more on rock type than drilling method. Televiewer data would have revealed finer detail if diamond drilling had been carried out, as it produces smoother walls. However, data were of good quality and major features could easily be identified.

It should be noted that these results and interpretations are representative of conditions in the shallow bedrock. As borehole depth in rock rarely exceeded ~20 m, it was not possible to assess variation of structural and hydraulic properties with depth. To do this would require logging at least one or two deep boreholes (50~100 m of open rock) in each context, as was done with the St-Germain borehole (135 m of open rock). In the latter, nearly 100 more features were interpreted than in the nearest shallow borehole, PO-14 (14.5 m open rock). In the St-Germain well, three broken zones, a flowing feature at 90.3 m depth, and numerous joints were observed.

4.2 Downhole logging results

All phases of the downhole logging were successful in collecting a suite of information that identified variations in lithological, hydrogeological, and structural conditions in the boreholes.

Hydrogeologically, it is recommended to continue logging with the natural gamma and high-resolution temperature tools within the metal casing, in addition to the open rock. The logs identify changes in unconsolidated materials, and also associated changes in fluid temperature caused by groundwater movement behind the casing wall. This is particularly important right at the overburden/bedrock contact to infer sources of fluid flow when performing flowmeter testing near the casing/bedrock contact.

The flowmeter used for this testing is highly sensitive, capable of detecting natural head differences (ambient flow) between 0.03 USGal/min (0.11 L/min) and 1.00 USGal/min (3.78 L/min). However, ambient flow was not recorded in any of the boreholes tested. Therefore, a very sensitive flowmeter, such as the thermal pulse tool used here, or an electromagnetic flowmeter instrument, is recommended for future testing since most wells of this region are not highly productive. Although a number of open fractures were found to flow under pumped conditions, flowmeter and fluid temperature data indicated that a large proportion of the fluid recovered during the pumping tests was entering the borehole at the base of the casing (thus coming from the surficial deposits or from the bedrock/surficial deposit contact). Similar results have been recorded in another regional project in the Saguenay region of Québec, by a research team from UQAC (Richard et al., 2012), in which case they deduced that the “defective” well casings were not properly sealed.

Geologically, it was noted that the natural gamma, magnetic susceptibility, and full waveform sonic (velocity) logs, when interpreted together, were particularly effective in distinguishing variations in lithology, and thus, potential zones of weakness leading to groundwater pathways between rock units.

Gamma logs were also very effective at defining the depth of the overburden/bedrock contact zone through the casing, and adjusting lithological contacts in uncored holes.

Structural orientations interpreted from the ATV images were successfully used to look at the variation in strike direction and dip of features based on structure type (broken zone, open and closed features). This outcome shows the importance of setting up a classification scheme that considers the project objectives in advance of performing the image analysis. The ATV images also revealed a relative degree of metamorphism or folding in the bedrock units based on the degree of dip in the beds.

Although the televiewer images show varying degrees of deformation through moderate-to-steeply dipping beds that often undulate (resulting in a distorted sinusoid in the unwrapped ATV image), clear evidence of bedrock movement (e.g. faulting) is less apparent at the borehole scale. Only in borehole PO-09 at 9.5 m depth (3.5 m below top of bedrock), can an 18 cm vertical offset in a steeply dipping open feature be seen. Fine movements (subcentimetre scale) could not be discerned due to the wall roughness produced by the downhole hammer drilling method.

4.3 Structural analyses

Analysis of interpreted structural-log data showed four fracture sets with a common NNE to NE average strike direction that agrees well with the regional strike of the St. Lawrence Platform and Appalachians main structures. According to the pole-density plot for open features only (Figure 7), the likely hypothesis of an orthogonal fracture setting is being investigated. However, these results are preliminary, as our initial conclusions rely on borehole structural data from eleven shallow wells and one deep well. Similar analysis of in-well structural features will be performed separately for each geological context in future work.

5.0 Future Research

To support our conceptualization of the structural setting and hydrogeological regime of the study area, several key questions will need to be addressed through ongoing research:

- Considering that only a few flowing fractures were observed with the flowmeter under pumped conditions, should it be concluded that virtually none of the features identified as open in structural logs are actually connected to the regional fracture network? Is this regional setting analogous to that described by Berkowitz (2002), who comments: “... of a large number of fractures intersecting a well, only one or two actually transmit fluid”. If so, should we distinguish more clearly “apparently open” features vs. “effectively water-bearing” fractures by refining classification of “open” features?
- Are the initial structural interpretations applicable at the regional scale? In other words, do logged wells provide structural information that is statistically representative of the regional fracture network setting? To answer this, additional work, including in situ outcrop fracture mapping, is being carried out.
- Is there some scale beyond which the fracture network is analogous to an “equivalent porous continuum”, or does it exhibit scaling behavior? Though it is difficult to say with currently available data, it is an important issue, as “systems that exhibit scaling behavior do not possess any homogenization scale” (Berkowitz, 2002). Such scale effect in hydraulic response of the fracture network would result in difficulties inferring regional-scale hydraulic properties.

- Is there a way to assess how fracture setting changes with depth — a decreasing fracture presence or a progressive fracture closure (e.g. as in Boutt et al., 2010)? Can this depth-dependence of the structural setting be used to explain the decreasing trend with depth of hydraulic conductivity that was obtained by Laurencelle et al. (2011) for the study area? To do so, deeper wells would have to be available for investigation using borehole logging and, possibly, hydraulic testing with packers.
- What residual impacts are the Quaternary glaciations having on the structural setting of the study area? According to Neuzil (2011), hydromechanical effects of continental glaciations on groundwater systems are more complex than previously assumed and, among other factors, flexural loading should be taken into account in addition to direct loading when modeling induced stresses and resulting fracture-system behavior. Several studies show how these modifications to the stress field result in small scale rock failure (Boulton and Caban, 1995) during deglaciation and postglacial faulting later on (Adams, 1989). This topic will be further investigated in Ph.D. research by M. Laurencelle.

Continued research on these questions will lead to a better understanding of regional groundwater flow in the Montérégie Est area and provide useful inputs to the regional flow numerical modeling to be carried out by INRS-ETE.

6.0 Acknowledgements

The authors wish to thank the well owners for their assistance during the fieldwork. Special thanks to Dr. Denis Lavoie for his advice on related geological topics, and to Mathieu J. Duchesne for his review.

7.0 References

- Adams, J., 1989. Postglacial faulting in eastern Canada: nature, origin and seismic hazard implications. *Tectonophysics*, 163(3–4): 323-331.
- Baecher, G., 1983. Statistical analysis of rock mass fracturing. *Mathematical Geology*, 15(2): 329-348.
- Berkowitz, B., 2002. Characterizing flow and transport in fractured geological media: A review. *Advances in Water Resources*, 25(8-12): 861-884.
- Boulton, G.S. and Caban, P., 1995. Groundwater flow beneath ice sheets: Part II — Its impact on glacier tectonic structures and moraine formation. *Quaternary Science Reviews*, 14(6): 563-587.
- Boutt, D., Diggins, P. and Mabee, S., 2010. A field study (Massachusetts, USA) of the factors controlling the depth of groundwater flow systems in crystalline fractured-rock terrain. *Hydrogeology Journal*: 1-16.
- Clark, T.H., 1964a. La région de Sainte-Hyacinthe (moitié ouest). SIGEOM, Rapport Géologique 101: 148 p.
- Clark, T.H., 1964b. Région d'Upton. SIGEOM, Rapport Géologique 100: 39 p.
- Faure, S., 1995. Reconstitution des paleocontraintes tectoniques dans les Basses Terres du Saint-Laurent et les Appalaches du Québec et du Nord du Nouveau Brunswick, Université du Québec, 252 pp.
- Faure, S., Tremblay, A. and Malo, M., 2004. Reconstruction of Taconian and Acadian paleostress regimes in the Quebec and northern New Brunswick Appalachians. *Canadian Journal of Earth Sciences*, 41(5): 619-634.
- Globensky, Y., 1987. Géologie des Basses Terres du Saint-Laurent. Direction Générale de l'Exploration Géologique et minérale du Québec - Gouvernement du Québec, pp. 71.
- Goodman, R.E., 1976. *Methods of geological engineering in discontinuities rocks*. West, St. Paul, MN.
- Kulatilake, P.H.S.W. and Wu, T.H., 1984. Estimation of mean trace length of discontinuities. *Rock Mechanics and Rock Engineering*, 17(4): 215-232.
- Laurencelle, M., Morin, R., Lefebvre, R., Rivard, C., Paradis, D., Lavoie, D., Benoît, N., Carrier, M.A. and Beaudry, C., 2011. Initial characterization of fractures and hydraulic properties of the Montérégie Est rock aquifer system. In: *GeoHydro2011* (Editor), Water and Earth: The junction of Quaternary Geoscience and Hydrogeology, Quebec.
- MDDEFP, 2008a. Programme d'acquisition de connaissances sur les eaux souterraines du Québec - Guide des conditions générales, premier appel de propositions. Gouvernement du Québec, 19 p., ISBN: 978-2-550-53934-6.
- MDDEFP, 2008b. Programme d'acquisition de connaissances sur les eaux souterraines du Québec - Guide du demandeur. Gouvernement du Québec, 8 p., ISBN : 978-2-550-53933-9.

- Neuzil, C.E., 2011. Hydromechanical effects of continental glaciation on groundwater systems. *Geofluids*: no-no.
- Park, H.J. and West, T.R., 2002. Sampling bias of discontinuity orientation caused by linear sampling technique. *Engineering Geology*, 66(1–2): 99-110.
- Priest, S.D., 1993. *Discontinuity analysis for rock engineering*, London.
- Richard, S.K., Chesnaux, R. and Rouleau, A., 2012. Estimation et analyse de la transmissivité des aquifères de type roc fracturé dans la région du Saguenay-Lac-Saint-Jean, Québec, Colloque du 80e Congrès de l'Acfas: Les connaissances sur les eaux souterraines régionales : acquisition et transfert. GRIES-RQES, Montreal, Canada.
- Rocher, M., Tremblay, A., Lavoie, D. and Campeau, A., 2003. Brittle fault evolution of the Montréal area (St Lawrence Lowlands, Canada): rift-related structural inheritance and tectonism approached by palaeostress analysis. *Geological Magazine*, 140(02): 157-172.
- Roller, K. and Trepmann, C.A., 2011. Stereo32 software. Ruhr-Universität Bochum, Bochum, Germany.
- Roy, D.W., Verreault, N. and Pino, D.S., 2011. Correction de Terzaghi, Graduated Course, Analyse Structurale, Université du Québec à Chicoutimi.
- Slivitzky, A. and St-Julien, P., 1987. Compilation géologique de la région de l'Estrie-Beauce. Direction Générale de l'Exploration Géologique et minière du Québec - Gouvernement du Québec. Report MM 85-04.
- Terzaghi, R.D., 1965. Sources of error in joint surveys. *Geotechnique*, 15 (3): 287-304.
- Williams, H., 1979. Appalachian Orogen in Canada. *Canadian Journal of Earth Sciences*, 16(3): 792-807.

Appendix I – Geophysical Log Background

Appendix I provides background information on the downhole logging methods used in the Montérégie Est area, and Appendix II presents the interpreted figures of the log suites.

Gamma Methods

Natural gamma logging detects the presence of naturally occurring or man-made radioactive isotopes. The most common naturally-occurring isotopes in rock and soil are potassium (K), uranium (U), and thorium (Th), the most common being potassium in rock forming minerals.

Natural gamma logging tools measure radioactivity by converting gamma rays (photons) emitted from the formation into electronic pulses using a scintillator crystal (detector) in the tool. For total count gamma logging, it is sufficient to count the total number of pulses per second. In spectral gamma logging, the amplitude of the pulse is needed to determine whether the gamma ray energy lies within the range corresponding to the windows for K, U, or Th. At each depth interval, a spectrum (counts per second versus energy levels) is built from the amplitudes of the incident gamma particles. The counts from each window can be later processed to calculate the weight percent of K, U, and Th in the formation using curves determined at downhole calibration facilities.

Radioactive decay is statistical in nature and photon emission follows a Poisson's distribution. The standard deviation of the count number will be its square root. The accuracy of the measurement is greatest at high count rates over slower logging speeds. Therefore it is preferable to maintain a very low logging speed.

When overburden units are logged, relative abundances of potassium, and especially uranium and thorium will generally be low, if present. This is particularly true in finer grained soils where the heavier elements were dropped out of suspension earlier in the sedimentary process, although exceptions exist. In soils, therefore, gamma energy is generally more present in the lower ranges due to scattering, and can be used as a relative indicator of grainsize. A denser formation will cause the natural radiation to be attenuated more quickly, therefore coarser grain sizes will tend to have a lower count rate, while softer soils with finer grain sizes (silt/clay) and higher porosity will tend to record higher count levels.

Electromagnetic Induction Methods

The **apparent conductivity** logging tool uses an alternating current of 40 kHz AC in a dipole transmitter to generate a magnetic field which induces electric fields in the formation. A dipole receiver in turn measures the responding signal, whose quadrature phase is proportional to the conductivity of the materials intersected by the borehole. Additional coils are used to focus the current out into the borehole to reduce the tool's sensitivity to the borehole fluid and improve its vertical resolution.

In soil and rock logging, the apparent conductivity measured is a bulk conductivity, meaning that the grains and pore water both contribute to the total conductivity values. If the porewater is saline or otherwise conductive (e.g. leachate contamination), this will overwhelm the conductivity of the soil/rock matrix. In absence of conductive porewater, the conductivity tool provides a method of

identifying variation in stratigraphic units, and tends to mirror the trends of the natural gamma log, where fine grained materials tend to be more conductive than coarse.

The **magnetic susceptibility** measurement is the ratio between the primary magnetic field and the in phase component of the magnetic field produced by the host material. Although traditionally used for downhole mineral exploration due to its sensitivity to magnetic minerals (e.g. magnetite, ilmenite, pyrrhotite), the susceptibility tool has been shown to be extremely useful for lithological logging purposes in unconsolidated sediments and sedimentary rocks of low susceptibilities (McNeill et al., 1996).

Although these inductive tools are quite similar, lithological mapping requires a very sensitive magnetic susceptibility logger (in the sub-parts-per-thousand SI) with a high degree of temperature compensation. Therefore, two induction tools are used for the conductivity and susceptibility logging, with slightly different coil configurations and temperature compensation electronics.

Note that the unit for magnetic susceptibility is most commonly SI, but some texts also use the unit CGS. The conversion between these two systems is:

$$SI = 4\pi * CGS.$$

Fluid Logging Methods

Temperature

The GSC conducted borehole research in the late 70's and early 80's on techniques for high resolution temperature measurements on the order of 0.0001°C. The purpose was to investigate the feasibility of recording temperature gradients in fluid-filled boreholes which would reflect the intersected lithology (Bristow and Conway, 1984). The GSC has recently redeveloped a temperature tool based on the original GSC design which could also potentially identify small temperature changes indicative of fluid movement behind casing for groundwater studies.

To be effective, the temperature tool must be the first probe to enter the borehole after the fluid has been able to stabilize for at least 24 hours, and the log must be recorded in the down direction. Slow logging speeds prevent mixing of the fluid ahead of the probe and allow time for the thermistor to react to slight changes in temperature. Gradient calculations (dT/dz) assist in identifying zones where fluctuations occur over very small changes in temperature.

References:

Bristow, Q., and Conaway, J.G., 1984. Temperature Gradient measurements in boreholes using low noise high resolution digital techniques, Current Research, Part B, Geological Survey of Canada, Paper 84-1B, p.101-108.

McNeill, J.D., Hunter, J.A., and Bosnar, M., 1996. Application of a borehole induction susceptibility logger to shallow lithological mapping, Journal of Environmental and Engineering Geophysics, Vol. 1, p. 77-90.

Heat Pulse Flowmeter

Many methods have been developed over recent decades to measure vertical fluid flow along an open borehole or well screen for groundwater applications. These methods have included impellers, tracer-release methods, thermal-pulse flowmeters, and electromagnetic (EM) flowmeters. Thermal and EM vertical component flowmeters are quite sensitive in low-flow conditions, permitting high-resolution measurement of the ambient vertical flow in natural or pumped borehole environments. Ambient flow measurements provide information on the direction of the vertical component of the hydraulic gradient and the location of hydraulically active features in fractured bedrock. Measurements made under artificial pumping conditions provide information on the relative differences in the permeability of targeted bedrock zones or fractures.

The heat pulse flowmeter used in these surveys (HFM-2293 manufactured by Mount Sopris Instrument Co.) is based on a US Geological Survey design to measure low-velocity flow environments (Hess, 1982, 1986). This flowmeter contains a heating grid with equidistant temperature sensors positioned a few centimetres above and below the grid. Rubber diverter petals centralize and seal the probe in the borehole, forcing the fluid to pass through a wire mesh over the heating grid and the sensors. When the tool is in position for a series of readings, a heat pulse is triggered by the user on a laptop computer. The grid heats a lens of water that moves up or down with the flow of the borehole fluid past either the upper or lower sensor. An amplifier detects the difference in temperature between the sensors, and converts the output to a frequency which is sent up the cable and recorded by the laptop. The software records the time elapsed between when the heat pulse was triggered and when the sensor records the peak temperature change, carried by the flow.

If natural flow is not detectable in the borehole (i.e. <0.110 L/min), artificial upward flow can be induced with a submersible pump to determine the relative flow drawn from permeable fractures. Flow rate must be carefully monitored every few minutes on surface using a graded container and a stopwatch, while water levels are measured in the borehole using a water level meter. This ensures the change in flow rate measured by the tool can be attributed to changes in hydraulic conductivity of the rock mass and not to changes in the pumping rate. The pump's flow rate must be carefully adjusted so it does not exceed the tool's upper limit of 3.78 L/min, and also to equalize the pumping rate with the recharge (i.e. no measurable drop in water level during the pumping). In non-hydraulically conductive boreholes, reaching stability is very difficult, and sometimes not possible. In these cases, the flow results are converted from a volumetric value, to a percentage of the total pumping rate measured simultaneously at the surface during the downhole flow measurement.

Flowmeter measurements are influenced by number of factors, including the construction and degree of development of a well, and the natural hydrogeological conditions: factors which can change over time. Logging conditions during the test will also influence the results. Proper sealing with the tool's rubber diverters is critical, as a poor seal caused by borehole wall enlargements (such as in fractures or washouts) will influence flow determinations. Collecting caliper and fluid temperature/fluid conductivity logs before flowmeter logging guides the selection of test intervals. Allowing sufficient time for the fluid to settle after moving the tool in the borehole is also critical, particularly in wells with very low ambient flows.

References:

Hess, A. E., 1982. A heat-pulse flowmeter for measuring low velocities in boreholes, U.S. Geological Survey Open-File Report 82-699, U.S. Geological Survey, Reston, Virginia.

Hess, A. E., 1986. Identifying hydraulically conductive fractures with a slow-velocity borehole flowmeter, *Canadian Geotechnical Journal*, 23:69-78.

Imaging Methods

Acoustic Televiewer

Televiewers provide a method of imaging the inside of the borehole wall in very high resolution, either using ultrasonic pulses (acoustic televiewer, ATV), or color digital scans (optical televiewer, OTV). The ATV transmits a pulse from a fixed transducer and a rotating focusing mirror, and records the amplitude and traveltime of the signal reflected by the borehole wall. The ATV used in these surveys (the ABI40, manufactured by Advanced Logic Technology SA.) records the entire reflected wavetrain, and processing algorithms allow the software in real time to determine the first reflection from the tool's acoustic window, the bedrock wall, and all other subsequent reflections.

Line scans of the borehole wall are collected in intervals as small as 1mm, and at a resolution as high as 288 pixels/revolution. The number of pixels per degree will depend on the diameter of the borehole. To collect images this detailed, the tool must be run very slowly (~1m/min) however a slight decrease in quality (i.e. 2mm intervals and/or fewer pixels/rev) can allow for a faster logging speed (~2-3m/min).

The tool is equipped with an APS544 orientation sensor, containing a 3-axis magnetometer and 3 accelerometers, to constantly resolve magnetic north and the tilt of the tool. Each line scan contains the direction of magnetic north, and also the tilt of the borehole at that depth. The tool can resolve azimuth with an accuracy of 1°, and tilt to an accuracy of 0.5°. When the traveltime and amplitude images are imported into processing software, they can be oriented to magnetic north (or to the high side of the borehole in the case of inclined borings). Once the dip and dip direction of structural features are interpreted, they can be corrected for any tilt of the borehole from vertical.

Centralization is key in the collection of high quality images, particularly with the ATV. The tool is kept centered in the borehole with the use of two or more bowspring arm centralizers, made of non-magnetic material, fixed to the tool's housing.

The ATV's traveltime image can be processed to build a 360° caliper of the borehole shape. This can then serve as a mesh around which the amplitude image can be draped to create a 3D image of the borehole. Features such as open fractures and washouts can be better visualized using this technique.

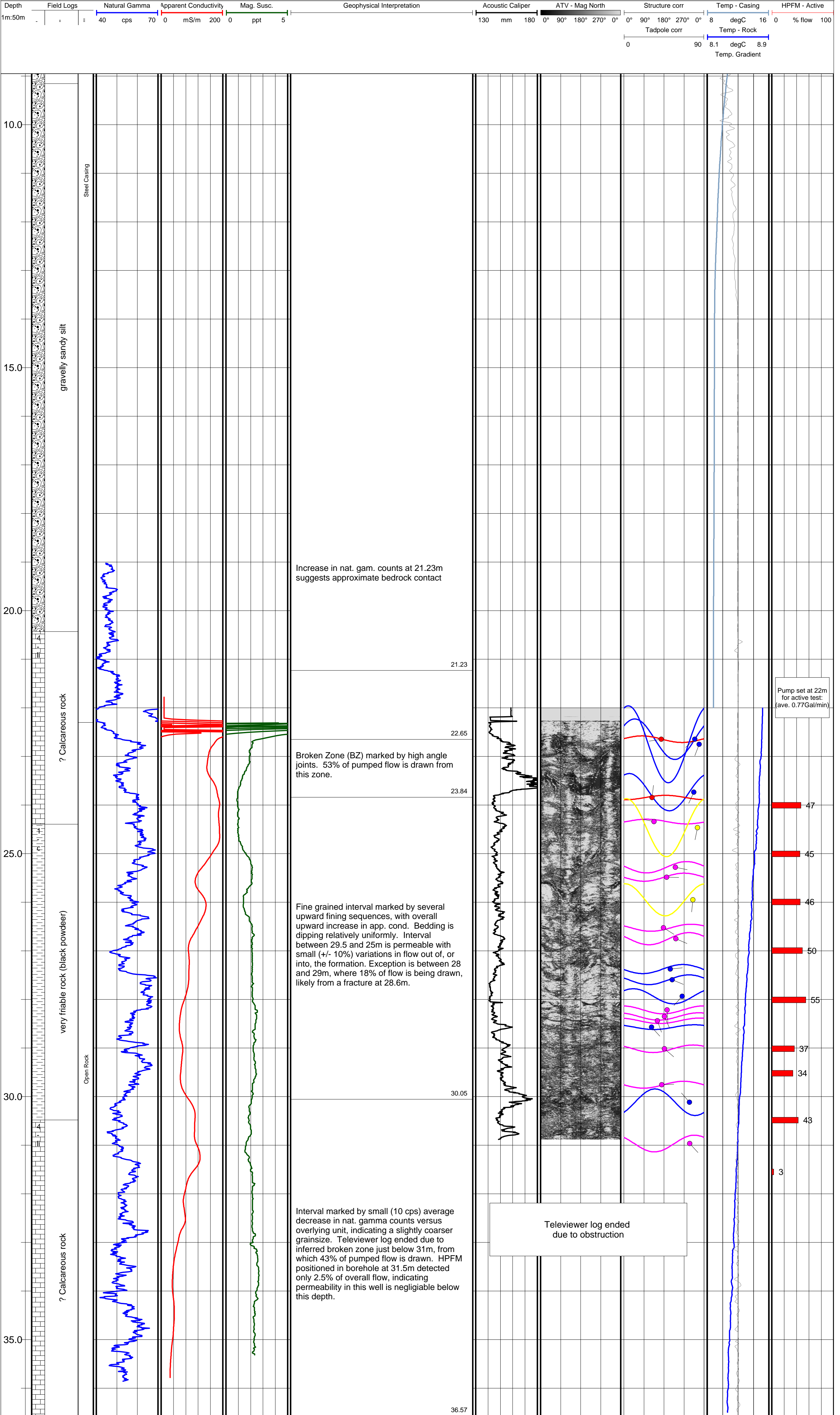
Appendix II – Geophysical Logs

Borehole: PO-02
Location: Bromont, QC
Project: Aquifer Assessment
Study Area: Montérégie-Yamaska

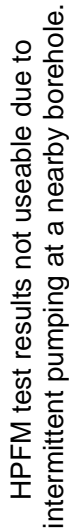
Easting: 680 245 m
Northing: 5 018 939 m
UTM Zone: 18
Datum: WGS84

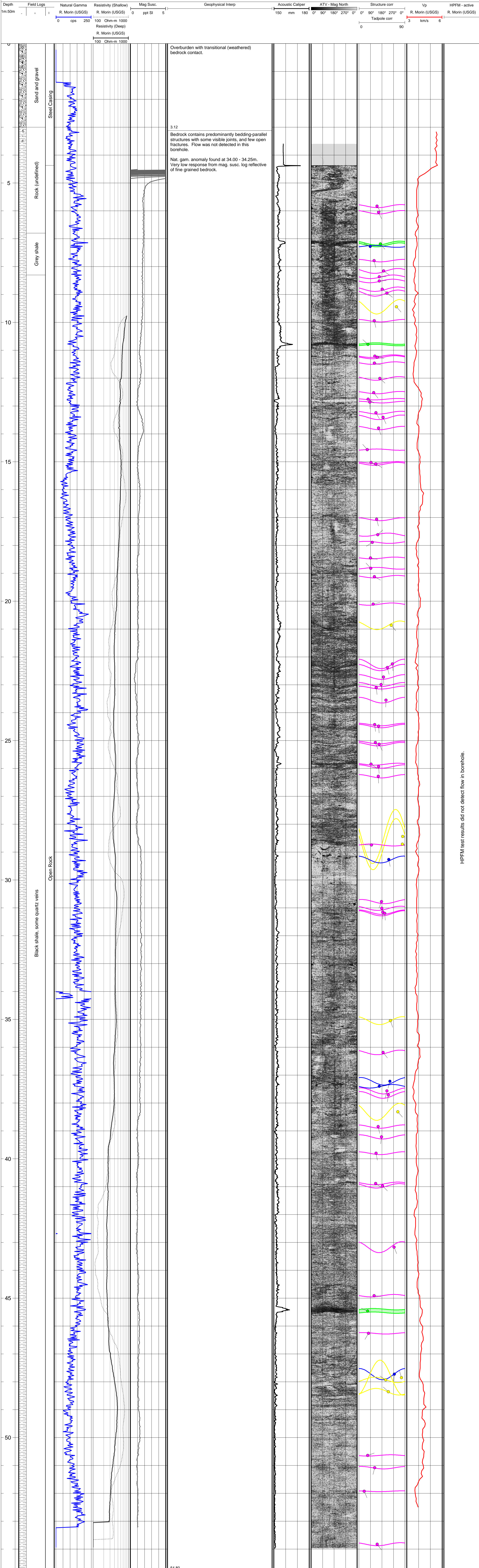
Date Drilled: Sept 30, 2011
Depth Drilled: 36.6 m
Method: DH hammer (ODEX)
Diameter: 14.0cm (rock), 15.9cm (casing)

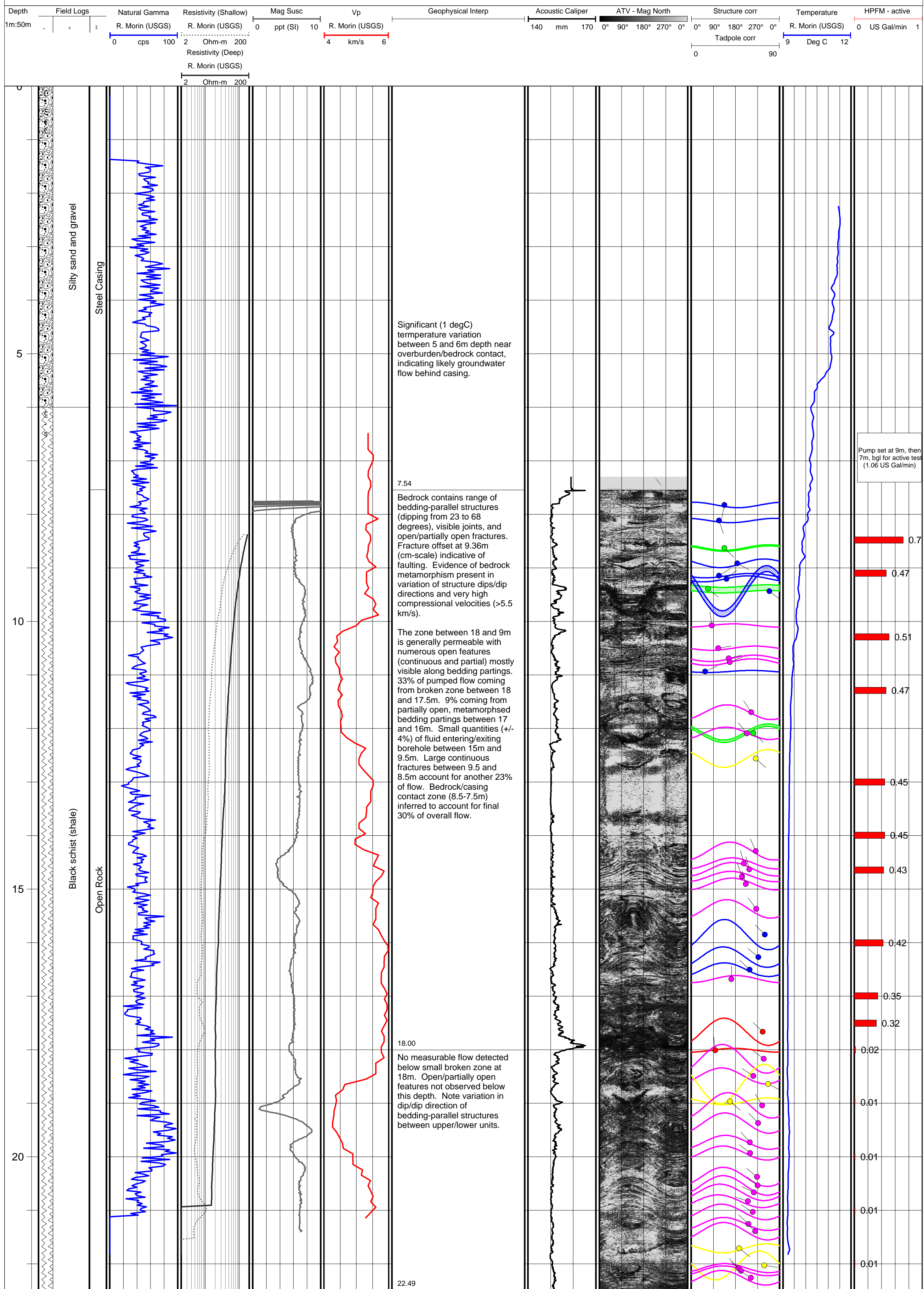
Date Logged: October 13, 2011
Piezometric
Water Level: 1.55m (bgl)



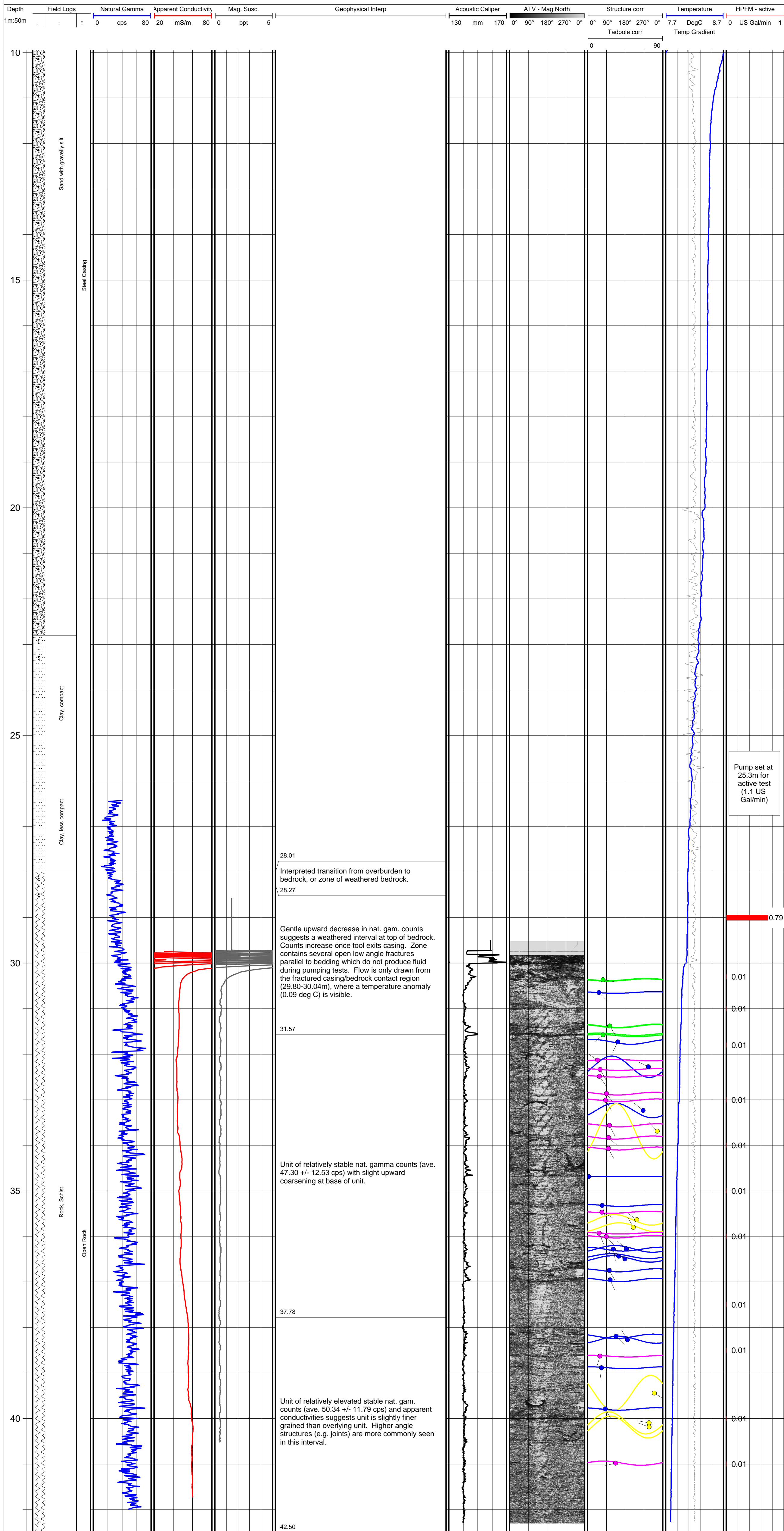
Date Drilled:	Oct 18, 2010	Date Logged:	Oct 18, 2010
Depth Drilled:	24.40 m	Piezometer:	None
Method:	Downhole Hammer	Water Level:	None
Diameter:	152mm (rock), 159mm (Casing)		







Date Logged: Oct 17, 2011
Piezometric
Water Level: 6.04 m bgl
(casing)

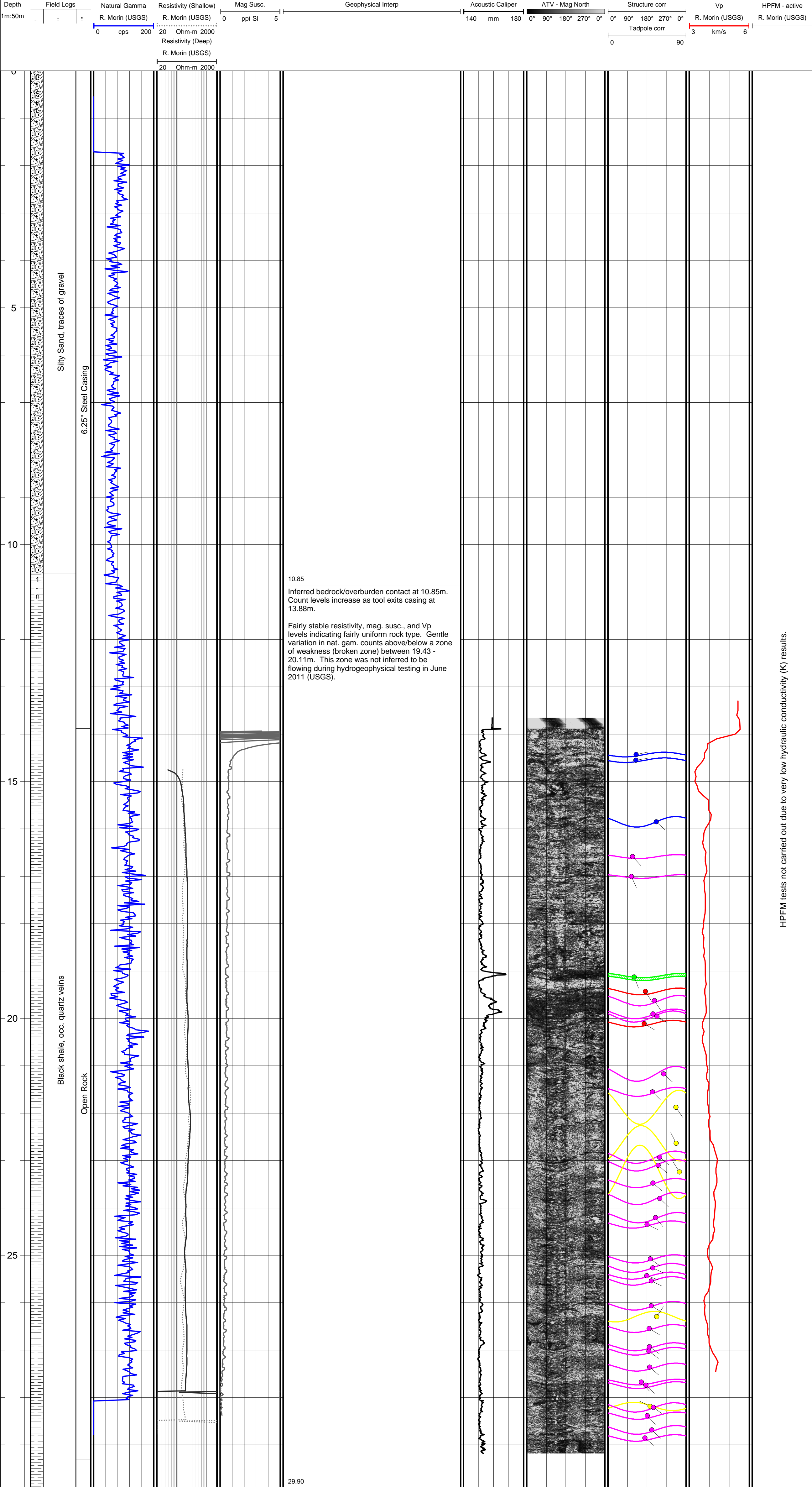


Borehole: PO-15
Location: St. Simon, QC
Project: Aquifer Assessment
Study Area: Monteregie-Yamaska

Easting: 668 090 m
Northing: 5 060 880 m
UTM Zone: 18
Datum: WGS84

Date Drilled: Nov 10, 2010
Depth Drilled: 29.9 m
Method: Downhole Hammer
Diameter: 152mm (rock), 159mm (casing)

Date Logged: Oct 18, 2011
Piezometric
Water Level: 3.15 m bgl



Silty Sand, traces of gravel

6.25" Steel Casing

Black shale, occ. quartz veins

Open Rock

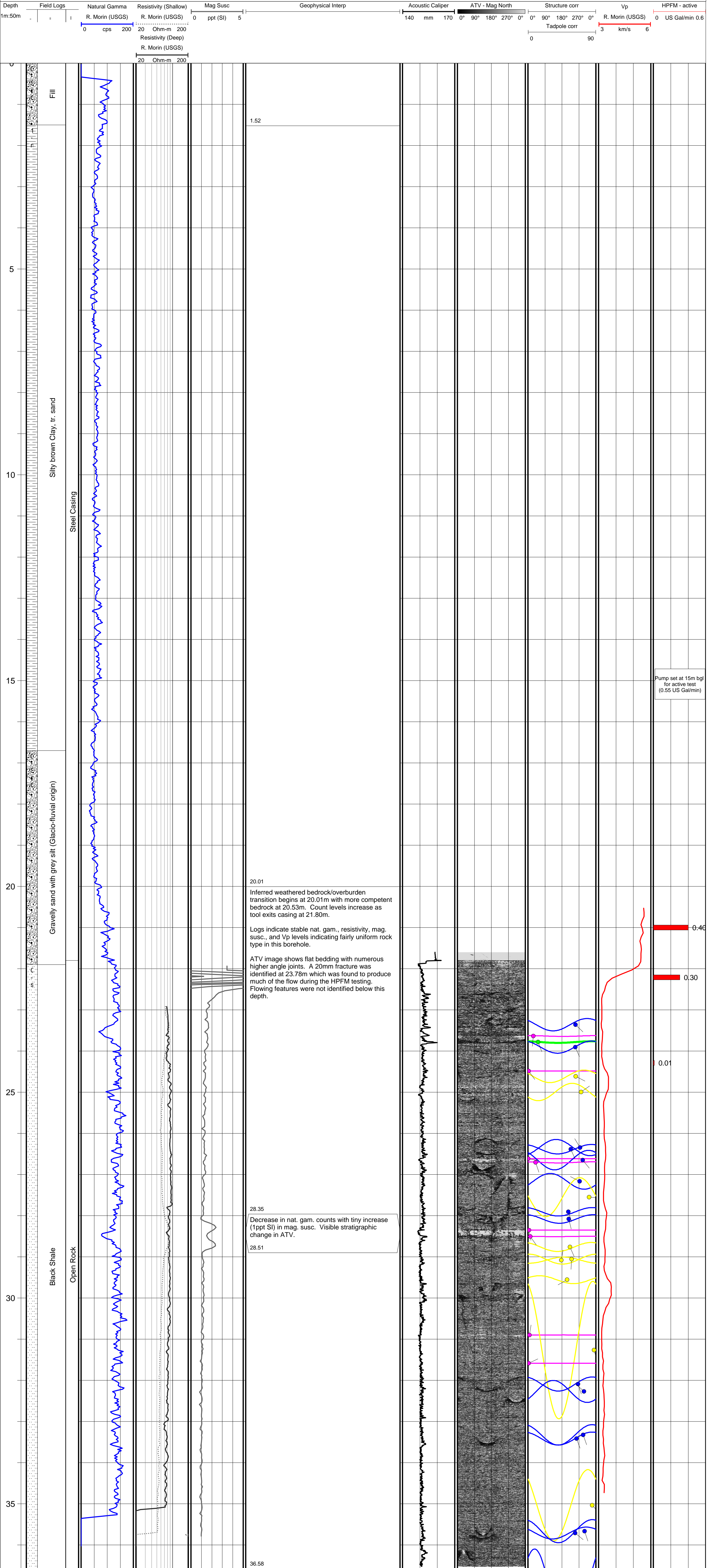
10.85

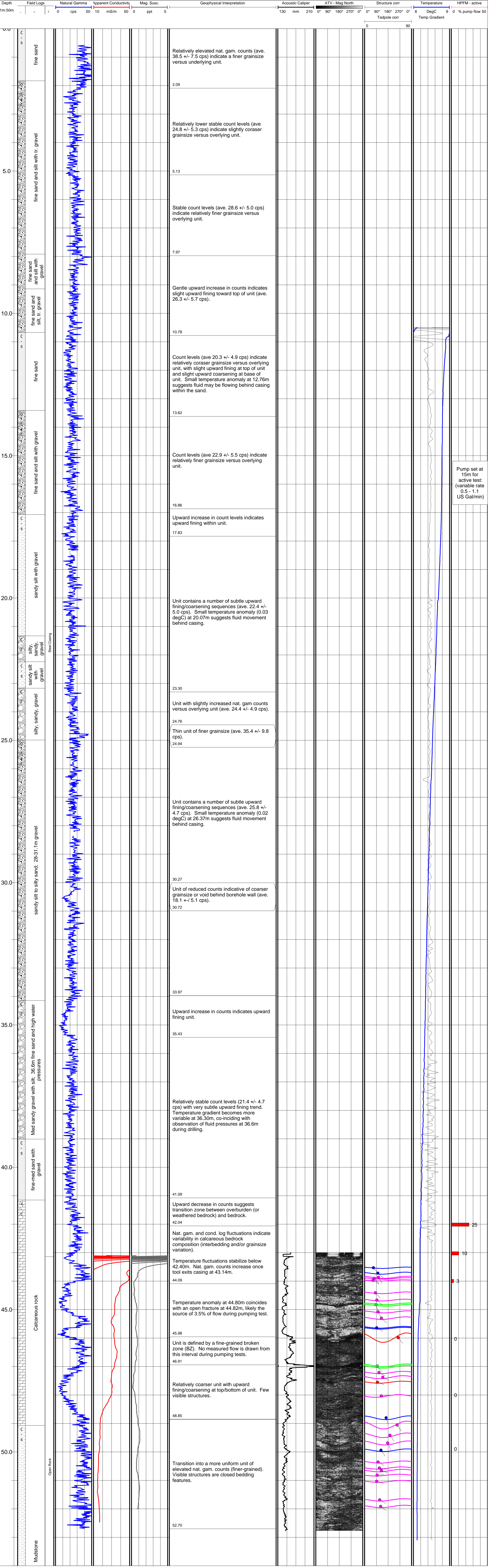
Inferred bedrock/overburden contact at 10.85m. Count levels increase as tool exits casing at 13.88m.

Fairly stable resistivity, mag. susc., and Vp levels indicating fairly uniform rock type. Gentle variation in nat. gam. counts above/below a zone of weakness (broken zone) between 19.43 - 20.11m. This zone was not inferred to be flowing during hydrogeophysical testing in June 2011 (USGS).

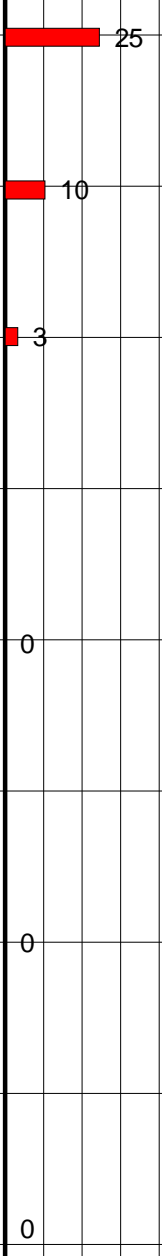
29.90

HPFM tests not carried out due to very low hydraulic conductivity (K) results.





Pump set at 15m for active test: (variable rate 0.5 - 1.1 US Gal/min)

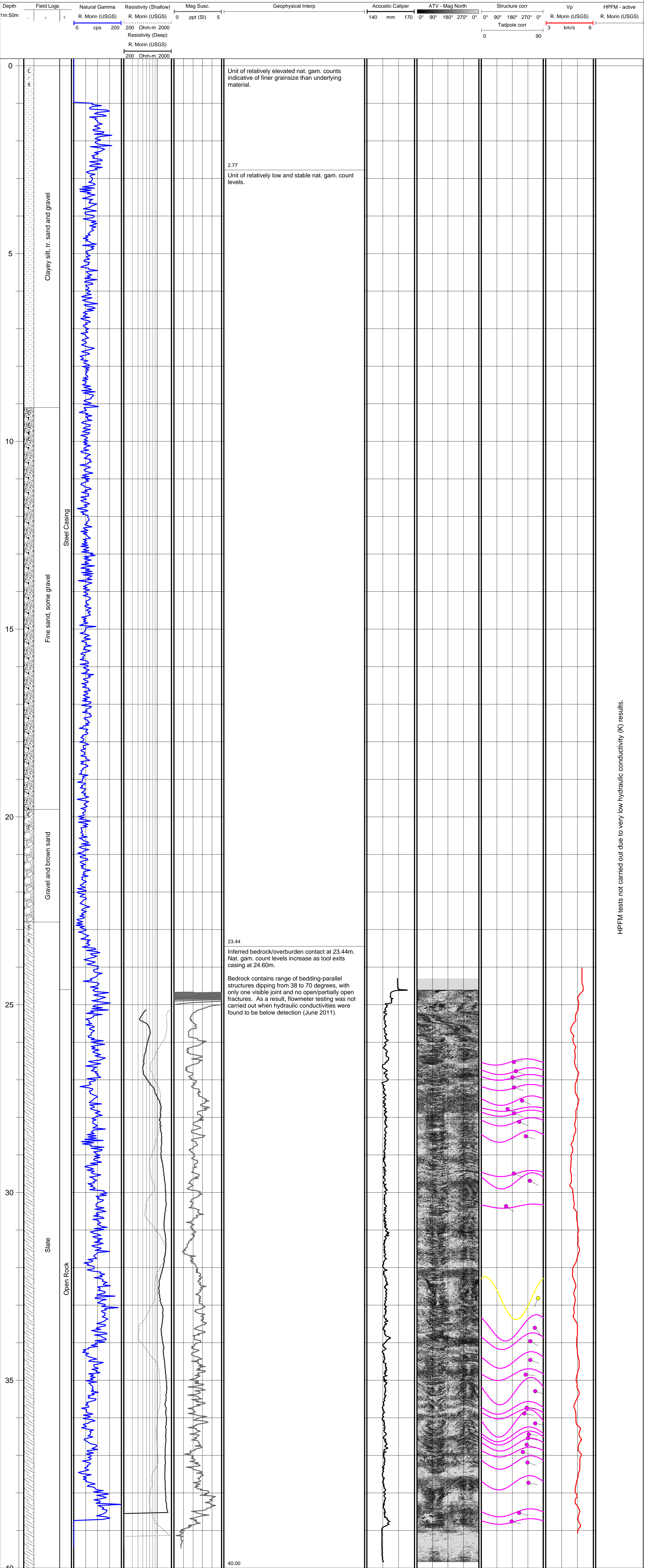


Borehole: PO-21
Location: Potton QC
Project: Aquifer Assessment
Study Area: Monteregie-Yamaska

Easting: 705 245 m
Northing: 4 992 684 m
UTM Zone: 18
Datum: WGS84

Date Drilled: Nov 5, 2010
Depth Drilled: 40.0 m
Method: Downhole Hammer
Diameter: 152mm (rock), 159mm (casing)

Date Logged: Oct 15, 2011
Piezometric
Water Level: 18.25 m bgl



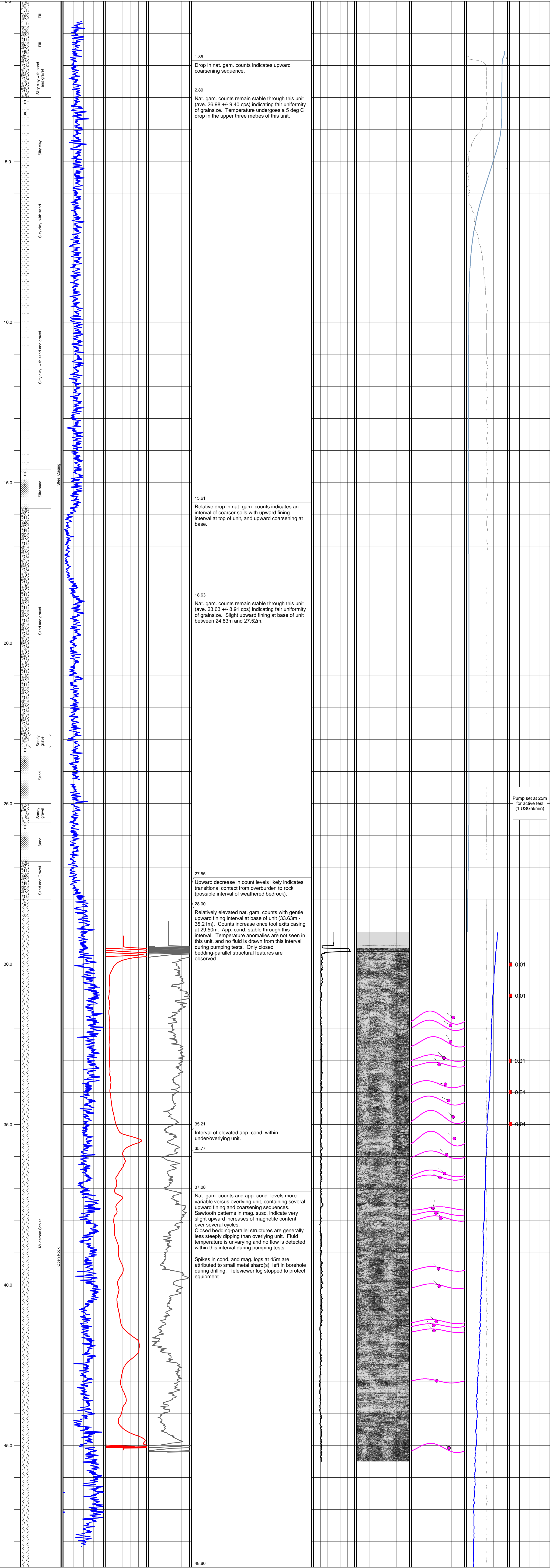
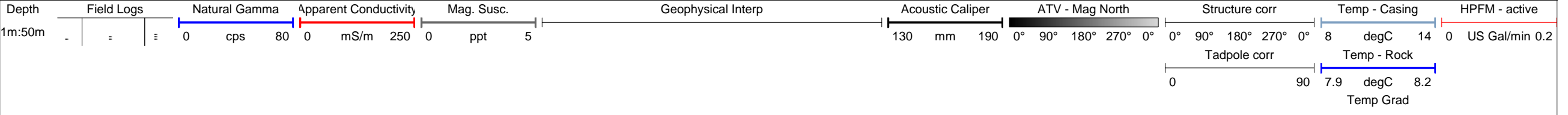
HPFM tests not carried out due to very low hydraulic conductivity (K) results.

Borehole: PO-22
Location: Sutton, QC
Project: Aquifer Assessment
Study Area: Monteregie-Yamaska

Easting: 686 863 m
Northing: 4 995 568 m
UTM Zone: 18
Datum: WGS84

Date Drilled: Sept 26-28, 2011
Depth Drilled: 48.80 m
Method: DH Hammer (ODEX)
Diameter: 140mm (rock), 159mm (casing)

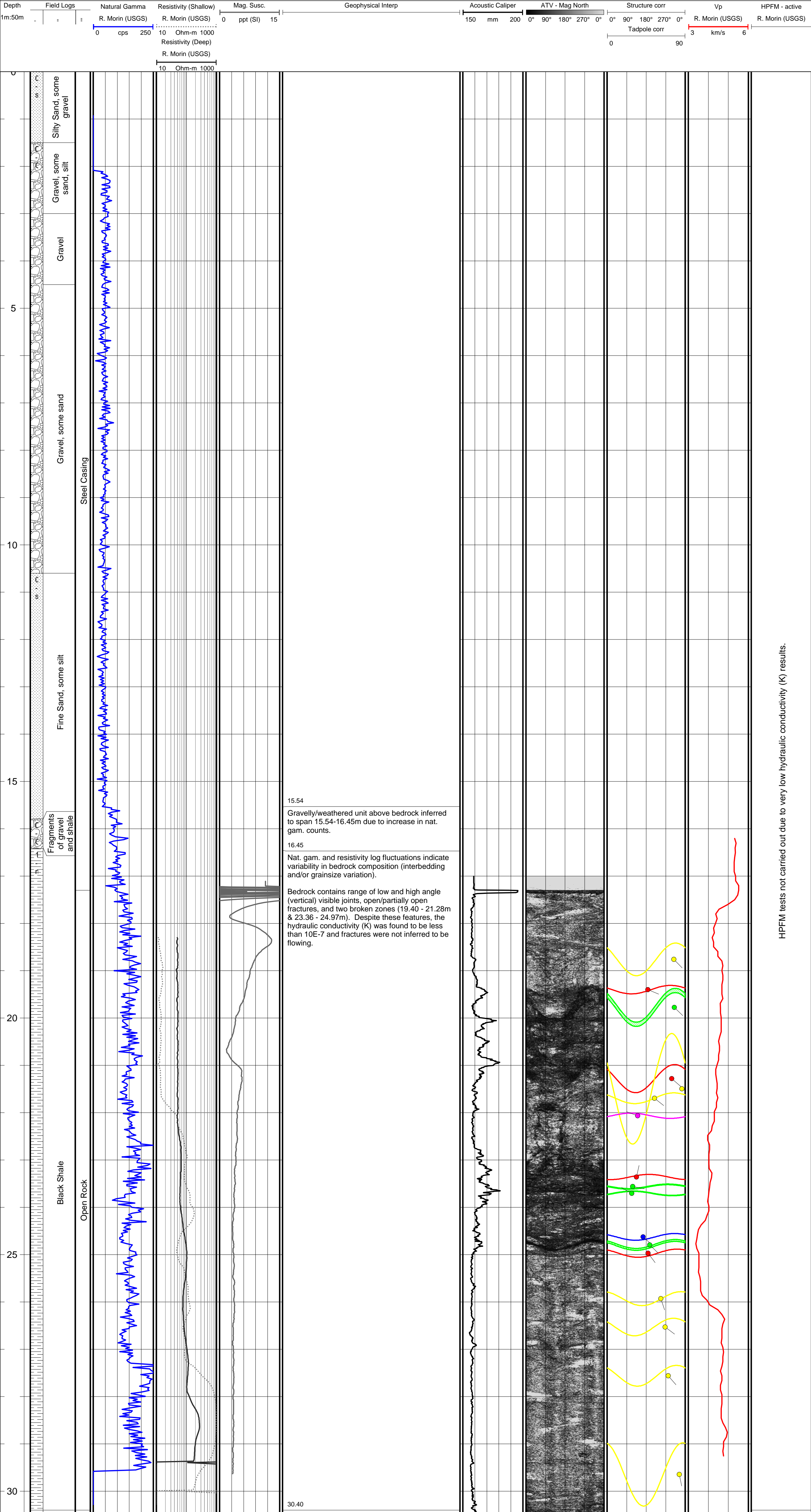
Date Logged: Oct 14, 2011
Piezometric
Water Level: -0.24 m (artesian)



Borehole: PO-24
Location: Eastman, QC
Project: Aquifer Assessment
Study Area: Monteregie-Yamaska

Easting: 711 247 m
Northing: 5 025 871 m
UTM Zone: 18
Datum: WGS84

Date Drilled: Oct 21, 2010
Depth Drilled: 30.40 m
Method: Downhole Hammer
Diameter: 152mm (rock), 159mm (casing)
Date Logged: Oct 15, 2011
Piezometric
Water Level: 0.79 m bgl



0

5

10

15

20

25

30

Silty Sand, some gravel

Gravel, some sand, silt

Gravel

Gravel, some sand

Fine Sand, some silt

Fragments of gravel and shale

Black Shale

Steel Casing

Open Rock

15.54

Gravelly/weathered unit above bedrock inferred to span 15.54-16.45m due to increase in nat. gam. counts.

16.45

Nat. gam. and resistivity log fluctuations indicate variability in bedrock composition (interbedding and/or grainsize variation).

Bedrock contains range of low and high angle (vertical) visible joints, open/partially open fractures, and two broken zones (19.40 - 21.28m & 23.36 - 24.97m). Despite these features, the hydraulic conductivity (K) was found to be less than 10E-7 and fractures were not inferred to be flowing.

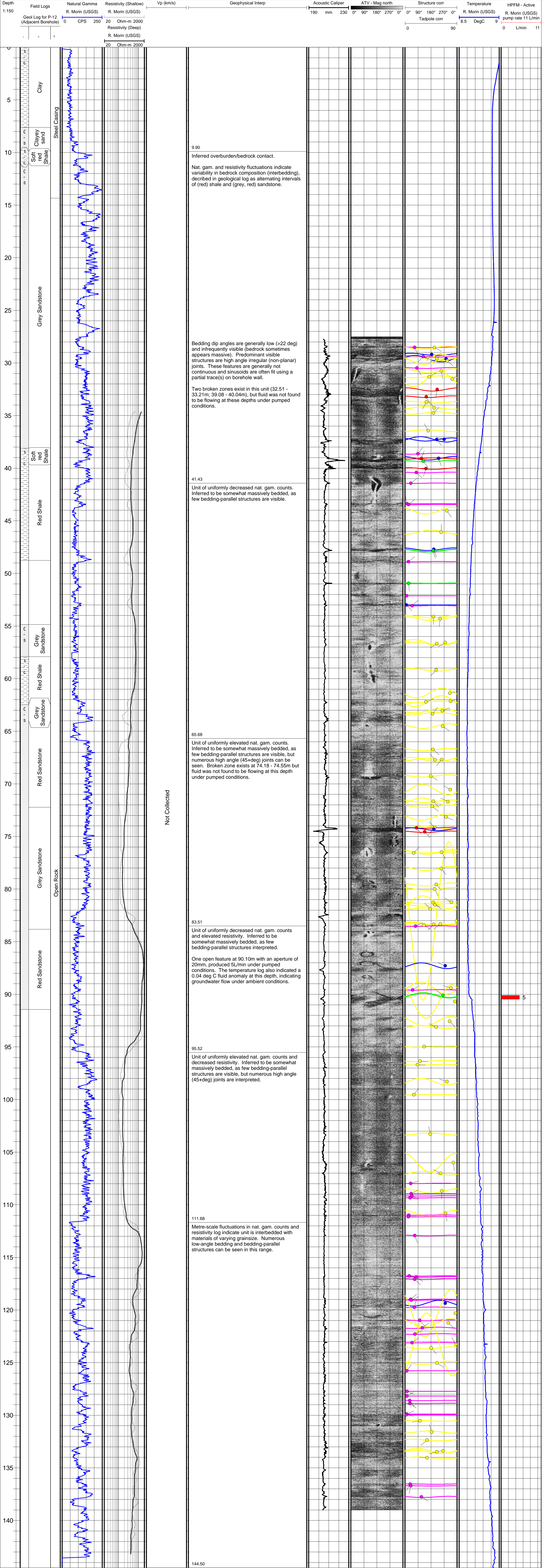
HPFM tests not carried out due to very low hydraulic conductivity (K) results.

Borehole: Puit de St. Germain
Location: St. Germain, QC
Project: Aquifer Assessment
Study Area: Monteregie-Yamaska

Easting: 692 107 m
Northing: 5 077 387 m
UTM Zone: 18
Datum: WGS84

Date Drilled: N/A
Depth Drilled: 146 m
Method: Percussion
Diameter: 203mm

Date Logged: Oct 18, 2011 (ATV)
Piezometric
Water Level: 28.29 m bgl

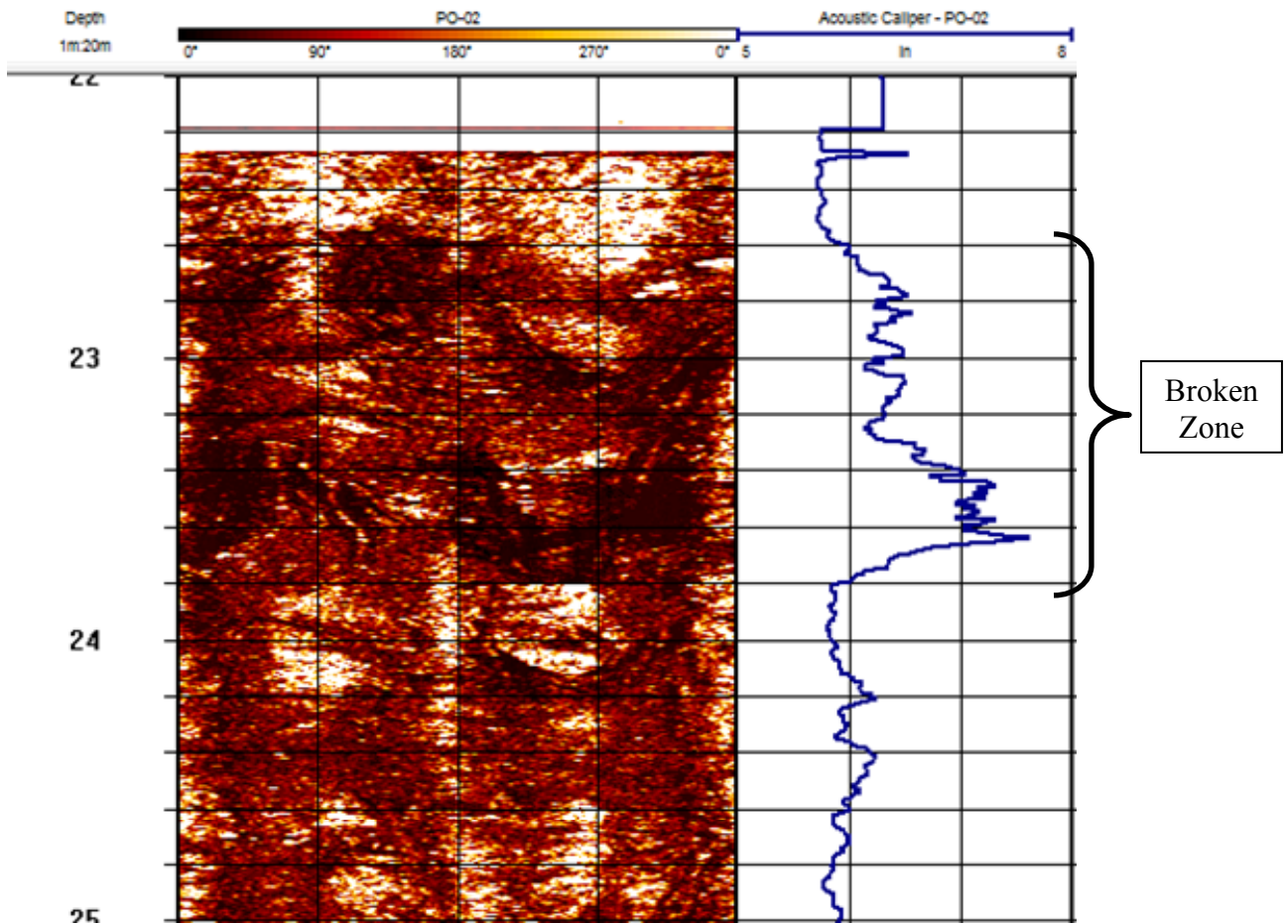


Appendix III – Structural Classifications

Televiewer Structural Classification

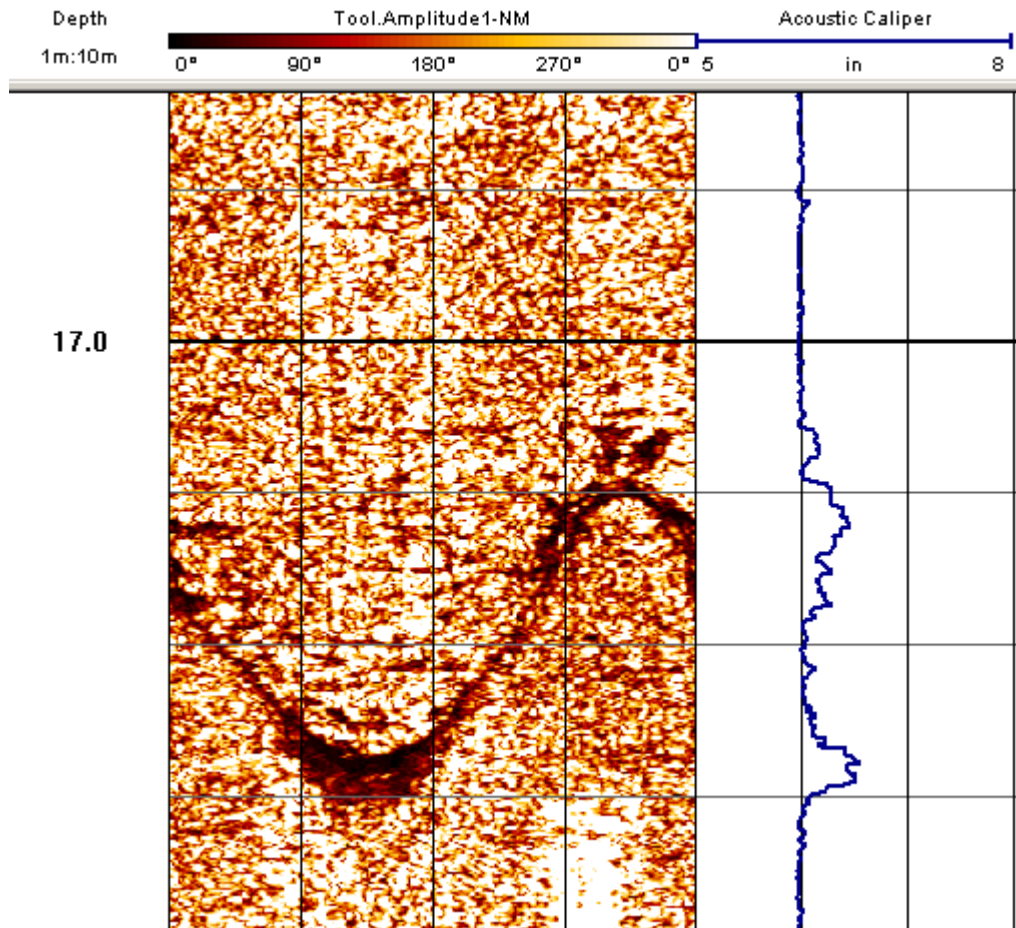
Type: Broken Zone

Sub-type: -



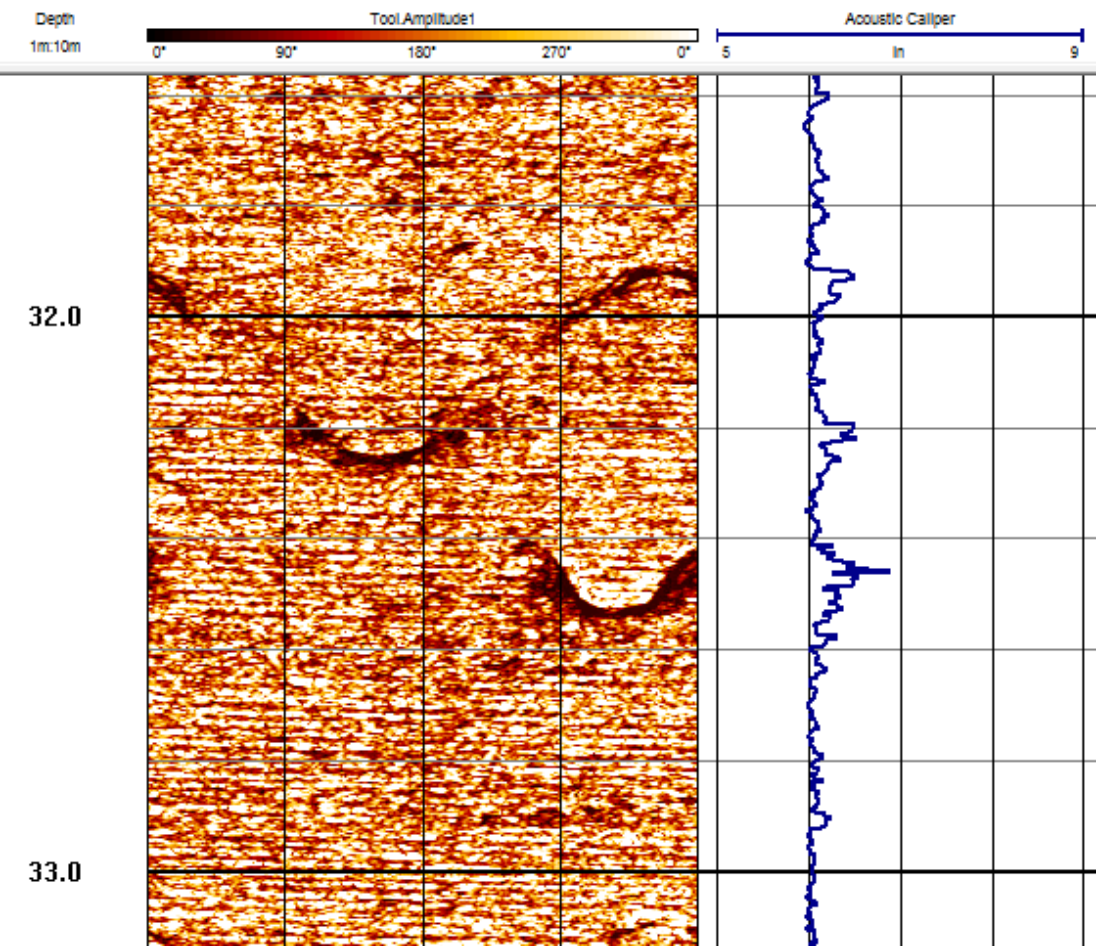
Note: The term 'Broken Zone' is generic, encompassing structures which are continuously fractured over 0.5 m or more, and exhibit significant aperture in the caliper log ($>1''$ beyond the nominal borehole diameter) at some point within the broken zone.

Type: Open Feature
Sub-type: Continuous fracture with aperture



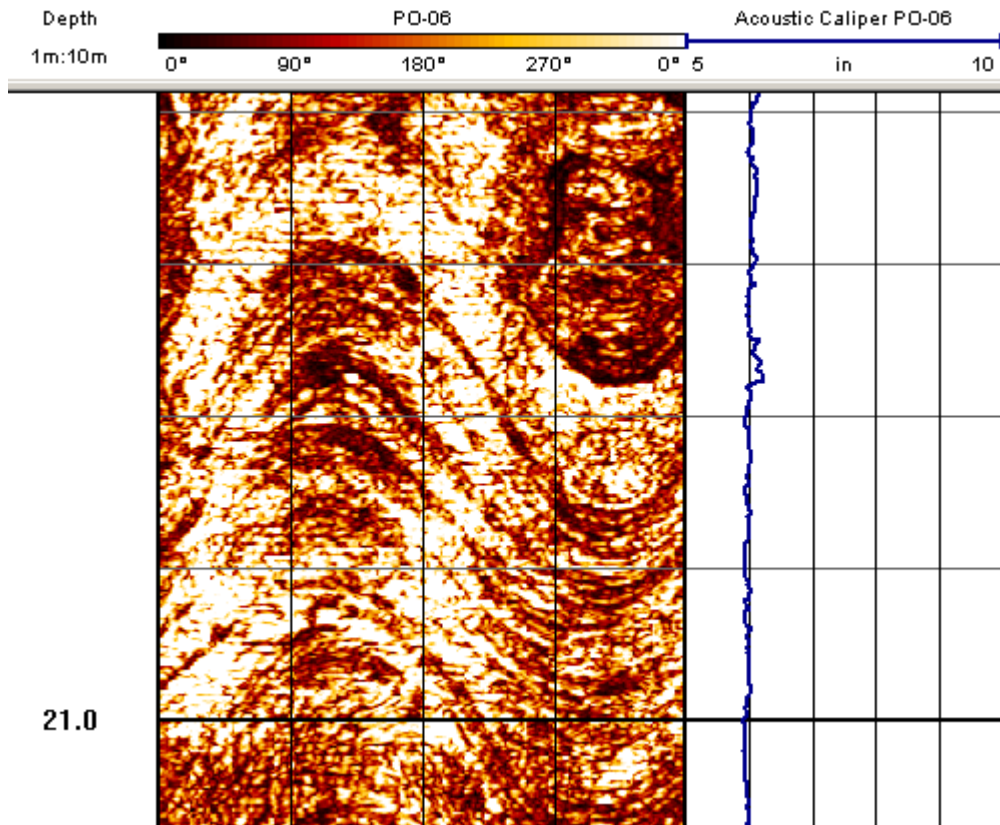
Note: The term 'Open Feature' is generic, encompassing structures which are open at least 10mm and exhibit aperture in the caliper log. This category includes features such as bedding partings and joints. Fractures may open preferentially along joints, but joints are difficult to determine solely from sonic images, therefore the term joint is not used here.

Type: Open Feature
Sub-type: Partial fractures with aperture



Type: Closed Feature

Sub-type: Parallel (e.g. bedding, foliation, etc)



Note: The term 'Closed Feature' encompasses structures which appear closed and don't exhibit aperture in the caliper log. This category includes:

Bedding
foliation,
fabric/schistosity



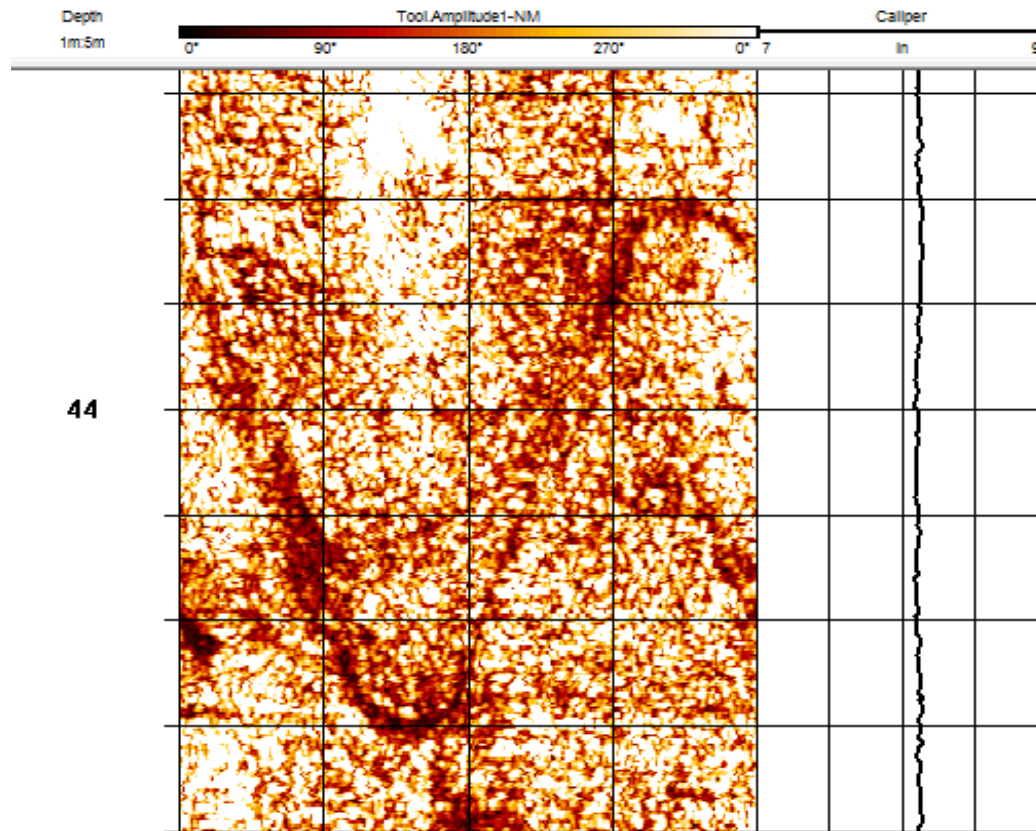
Closed parallel; shallow to moderately dipping features

closed (hairline) joints


Closed perpendicular; steeply dipping features

It can be difficult to determine the nature of closed features solely from acoustic images since a true color image, which helps distinguish geological features, is not available.

Sub-type: Perpendicular (e.g. high angle joints)



Tadpole Color Key

BZ		Broken Zone
OC		Open Continuous
OP		Open Partial
CP1		Closed Parallel
CPr		Closed Perpendicular